REPORT DOCUMENTATION PAGE		READ INSTRUCTIONS BEFORE COMPLETING FORM
1. REPORT NUMBER CI 79-43T	2. GOVT ACCESSION NO.	3. RECIPIENT'S CATALOG NUMBER
4. TITLE (and Subtitle) Determination of Stability and Control Derivatives for the Variable-Response Research Aircraft Using a Modified Maximum Likelihood Estimator		5. TYPE OF REPORT & PERIOD COVERED Thesis
		6. PERFORMING ORG. REPORT NUMBER
7. AUTHOR(s) 2LT Jean Michel Fernand		8. CONTRACT OR GRANT NUMBER(s)
9. PERFORMING ORGANIZATION NAME AND ADDRESS AFIT Student at Princeton University		10. PROGRAM ELEMENT, PROJECT, TASK AREA & WORK UNIT NUMBERS
11. CONTROLLING OFFICE NAME AND ADDRESS AFIT/CI WPAFB OH 45433		12. REPORT DATE September 1978
		13. NUMBER OF PAGES 132
14. MONITORING AGENCY NAME & ADDRESS(if different from Controlling Office)		15. SECURITY CLASS. (of this report) Unclassified
		15a. DECLASSIFICATION/DOWNGRADING SCHEDULE

16. DISTRIBUTION STATEMENT (of this Report)

Approved for Public Release, Distribution Unlimited

17. DISTRIBUTION STATEMENT (of the abstract entered in Block 20, if different from Report)

18. SUPPLEMENTARY NOTES

19. KEY WORDS (Continue on reverse side if necessary and identify by block number)

20. ABSTRACT (Continue on reverse side if necessary and identify by block number)

DD FORM 1473 EDITION OF 1 NOV 65 IS OBSOLETE
1 JAN 73

AD A063270

DDC FILE COPY

LEVEL

D D C
JAN 16 1979
C

79-43T

DETERMINATION OF THE STABILITY AND CONTROL DERIVATIVES FOR THE VARIABLE-RESPONSE RESEARCH AIRCRAFT USING A MODIFIED MAXIMUM LIKELIHOOD ESTIMATOR

by

2LT Jean Michel Fernand   Sep 78

Princeton University
School of Engineering and Applied Science
Department of Mechanical and Aerospace Engineering

Master's thesis

Submitted in partial fulfillment of the requirements for the degree of Master of Science in Engineering from Princeton University, 1978.

AFIT-CI-79-43T   140 p.

Prepared by:

Jean Michel Fernand

Jean Michel Fernand
2Lt. USAF

Approved by:

Robert F. Stengel

Professor R. F. Stengel

September, 1978
132 Pages

012 200

79 01 15 044

DETERMINATION OF THE STABILITY AND CONTROL DERIVATIVES FOR THE
VARIABLE-RESPONSE RESEARCH AIRCRAFT USING A MODIFIED MAXIMUM
LIKELIHOOD ESTIMATOR

79-43

BY: 2LT JEAN MICHEL FERNAND
Master of Science in Engineering from Princeton
University

ABSTRACT

A maximum likelihood estimation program was applied to
flight data for Princeton's Variable-Response Research
Aircraft to determine its primary stability and control
derivatives.   The control derivatives for the side-force
surfaces and the rudder were of special interest.   The
effects of measurement noise and process noise on parameter
identification also were studied.

This investigation showed that the maximum likelihood
estimation program used identifies derivatives which produce
close fits of the measured time histories. Standard
deviations of the derivatives computed from several time
histories indicate the quality of the estimates.   The
reduction in standard deviations when estimates were
separated by type and direction of control input time
history used indicates that derivative estimates are
affected by the assumptions inherent in the analytical model
and the signal-to-noise ratios of the data.   The method used
for identifying highly correlated derivatives also affected
the estimates obtained.   The final set of derivatives
determined in this research produced a good fit of the
measured data and several of the derivatives agreed well

i

with analog matching derivative estimates.

ii

REFERENCES

1. Shivers, James P. , Fink, Marvin P. , and Ware, George M. , "Full-Scale Wind-Tunnel Investigation of the Static Longitudinal and Lateral Characteristics of a Light Single-Engine Low-Wing Airplane," NASA TN D-5857, Jun. 1970.

2. Seckel, E. , and Morris, J. J. , "The Stability Derivatives of the Navion Aircraft Estimated by Various Methods and Derived From Flight Test Data," Rep. No. FAA-RD-71-6, Jan. 1971.

3. Suit, W. T. , "Aerodynamic Parameters of the Navion Airplane Extracted From Flight Data," NASA TN-D 6643, Mar. 1972.

4. Maine, R. E. and Iliff, K. W. , "A Fortran Program For Determining Aircraft Stability And Control Derivatives From Flight Data," TN-D-7831, Apr. 1975.

5. Etkin, B. , Dynamics of Atmospheric Flight, John Wiley and Sons, Inc. , New York, 1972.

6. Maine, R.E. , "Maximum Likelihood Estimation of Aerodynamic Derivatives For An Oblique Wing Aircraft From Flight Data," AIAA Paper 77-1135, Aug. 1977.

7. Stepner, D. E.,and Mehra, R. K. , "Maximum Likelihood Identification And Optimal Input Design For Identifying

Aircraft Stability And Control Derivatives," NASA CR-2200, Mar. 1973.

8. Iliff, K. W. and Taylor, L. W. , Jr. , "Determination of Stability Derivatives From Flight Data Using A Newton-Raphson Minimization Technique," NASA TN-D 6579, Mar. 1972.

9. Iliff, K. W, and Maine, R. E. , "Pratical Aspects of Using a Maximum Likelihood Estimator," AGARD CP 172, Nov. 1974.

10. Grove, R. D. , Bowles, R. L. , Mayhew, S. C. , "A Procedure For Estimating Stability And Control Parameters From Flight Test Data By Using Maximum Likelihood Methods Employing A Real-Time Digital System," NASA TN-D 6735, May 1972.

11. Balakrishnan, A. V. , Communications Theory. McGraw-Hill Book Co. , New York, 1968.

12. Brogan, W. L. , Modern Control Theory, Quantum Publishers, Inc. , New York, 1974.

13. Burgin, G. H. , "Two New Methods For Obtaining Stability Derivatives From Flight Test Data," NASA CR-96005, Sept. 1968.

14. Cannaday, R. L.,and Suit, W. T. , "Effects of Control Inputs on the Estimation of Stability and Control Parameters

of a Light Airplane," NASA Technical Paper 1403, Dec. 1977.

15. Mehra, R. K. , and Gupta, N. K. , "Status of Input Design Aircraft Parameter Identification," AGARD-CP-172, Nov. 1974.

16. Anon, ASCOP Special Goodyear PW Ground Station, Applied Science Corporation of Princeton, Oct. 1975.

17. Porter, F. H. , III, Flight Data Reduction, USAF Flight Test Center Publication T1'-700-1001, Jun. 1975.

18. Steers, S. T.,and Iliff, K. W. , "Effects of Time-Shifted Data on Flight-Determined Stability and Control Derivatives," NASA TN-D 7830, Mar. 1975.

19. Teper, Gary L. , "Aircraft Stability and Control Data," NASA CR-96008, Apr. 1969.

DETERMINATION OF THE STABILITY AND CONTROL

DERIVATIVES FOR THE VARIABLE-RESPONSE

RESEARCH AIRCRAFT USING A

MODIFIED MAXIMUM LIKELIHOOD ESTIMATOR

by

Jean Michel Fernand

Princeton University
School of Engineering and Applied Science
Department of Mechanical and Aerospace Engineering

Submitted in partial fulfillment of the requirements for the degree of Master of Science in Engineering from Princeton University, 1978.

Prepared by:

Jean Michel Fernand

Jean Michel Fernand

Approved by:

Robert F. Stengel

Professor R. F. Stengel

September, 1978

ABSTRACT

A maximum likelihood estimation program was applied to flight data for Princeton's Variable-Response Research Aircraft to determine its primary stability and control derivatives. The control derivatives for the side-force surfaces and the rudder were of special interest. The effects of measurement noise and process noise on parameter identification also were studied.

This investigation showed that the maximum likelihood estimation program used identifies derivatives which produce close fits of the measured time histories. Standard deviations of the derivatives computed from several time histories indicate the quality of the estimates. The reduction in standard deviations when estimates were separated by type and direction of control input time history used indicates that derivative estimates are affected by the assumptions inherent in the analytical model and the signal-to-noise ratios of the data. The method used for identifying highly correlated derivatives also affected the estimates obtained. The final set of derivatives determined in this research produced a good fit of the measured data and several of the derivatives agreed well

i

with analog matching derivative estimates.

iii

TABLE OF CONTENTS

LIST OF FIGURES

LIST OF TABLES

1. INTRODUCTION

Identification of aircraft parameters is becoming increasingly important in applying electronics technology to aircraft design for a number of reasons. Modern control design techniques rely on accurate aircraft aerodynamic models for best results. Computer analysis of aircraft stability, handling qualities, and mission effectiveness also depends on accurate aerodynamic models. Parameter identification from flight test data offers the advantage over analytical and wind tunnel results of determining stability and control derivatives of the actual aircraft in the flight regime of interest. The mechanization of parameter identification and the application of this procedure to Princeton's Variable-Response Research Aircraft (VRA) is the subject of this thesis.

The VRA is a specially modified Ryan Navion aircraft. Several studies have been made to determine its stability and control derivatives with varying success, including wind tunnel tests of the full scale aircraft (Ref 1), application of analytical methods, analog matching of test flight data (Ref 2), and maximum likelihood estimation from test flight

1 - 1

data (Ref 3). This study will make use of the Modified Maximum Likelihood Estimation program developed by Maine and Iliff (Ref 4) and similar in concept to the routine used in Ref 3.

1.1 Thesis Summary

The objectives of this thesis include the following:

. Identification of the primary longitudinal and lateral-directional stability and control derivatives for the VRA in its current configuration at a cruise condition of 105 KIAS.

. Identification of control derivatives for the modified rudder and the recently added side-force surfaces.

. Estimation of the effects of measurement and process noise on parameter identification.

In addition, the results obtained will reflect the efficiency and accuracy of the computer program used.

A total of 28 control input time histories from 2 test flights were used. The twenty lateral-directional time histories included aileron pulses, rudder doublets, and

1 - 2

side-force surface pulses and doublets. Estimation of longitudinal derivatives was restricted by the availability of only 8 suitable elevator doublet time histories. Dynamic measurement errors in the angle of sideslip and velocity instruments are documented; poor lateral accleration measurements and possibly erroneous angle of attack measurements also are noted.

The need for an improved analytical model is demonstrated by the seemingly nonlinear responses in roll, pitch, and yaw to control inputs. The large control inputs required by signal-to-noise ratio considerations add to this nonlinear aircraft behavior.

Improved control input design is needed to take full advantage of the maximum likelihood estimation technique. Control inputs that failed to excite all modes of motion resulted in large variances in the estimates of derivatives related to these modes. This result is demonstrated by the poor time history matches for aileron inputs. The VRA now has the capability for precise control inputs through its Microprocessor Digital Flight Control System. Tailored inputs would make the best use of existing controls in exciting all modes of interest.

1.2 Organization of Thesis

The remainder of this thesis is made up of 5 chapters and 3 appendices. Chapter 2 discusses the theory of maximum likelihood estimation. A linear, time-invariant analytical model is derived in detail. Next, the cost function used to evaluate the estimation is discussed. Finally the Modified Newton-Raphson minimization algorithm is described.

Chapter 3 discusses data acquistion and processing as well as preliminary inputs to the estimation program. The aircraft instrumentation is described in detail, and the steps in data processing are outlined. Specifying aircraft dimensions allows nondimensionalization of the estimated derivatives for more accurate comparisons. Initial estimates of the parameters to be identified are important to the success of the minimization algorithm.

Chapters 4 and 5 detail the results of lateral-directional and longitudinal derivatives determination. Initial estimates illustrate problems with the data and the analytical model. Steps are then taken to improve the quality of the estimates. Additional runs are made to add insight into problems experienced.

Chapter 6 summarizes the results of this research and

1 - 4

the recommendations for further research.

Appendices A and B tabulate the results of runs described in Chapters 4 and 5 and list several important averages. Appendix C lists the nomenclature used in this thesis.

2. THEORY OF PARAMETER ESTIMATION

Identifying aircraft parameters from test flights begins with three determinations:

. Selection of the analytical model.

. Identification of the cost function.

. Determination of an algorithm to minimize the cost function.

Choosing the appropriate analytical model, and thus, the parameters to identify in the equations of motion, may involve reducing the order of the model to a managable level and making simplifying assumptions to reduce the complexity of the model. A quantifiable index of performance, or cost function, permits optimization of the identification process and evaluation of the success of the process. Maximum likelihood estimation uses the log likelihood function of the parameters to be identified as the basis for its cost function. A numerical algorithm which reduces the cost function, allows digital computation of the parameter estimates with limited and/or no need for operator judgement. The Modified Newton-Raphson algorithm performs these functions. Figure 1 shows the relationship of these factors to the process of parameter estimation. Each of

2 - 1
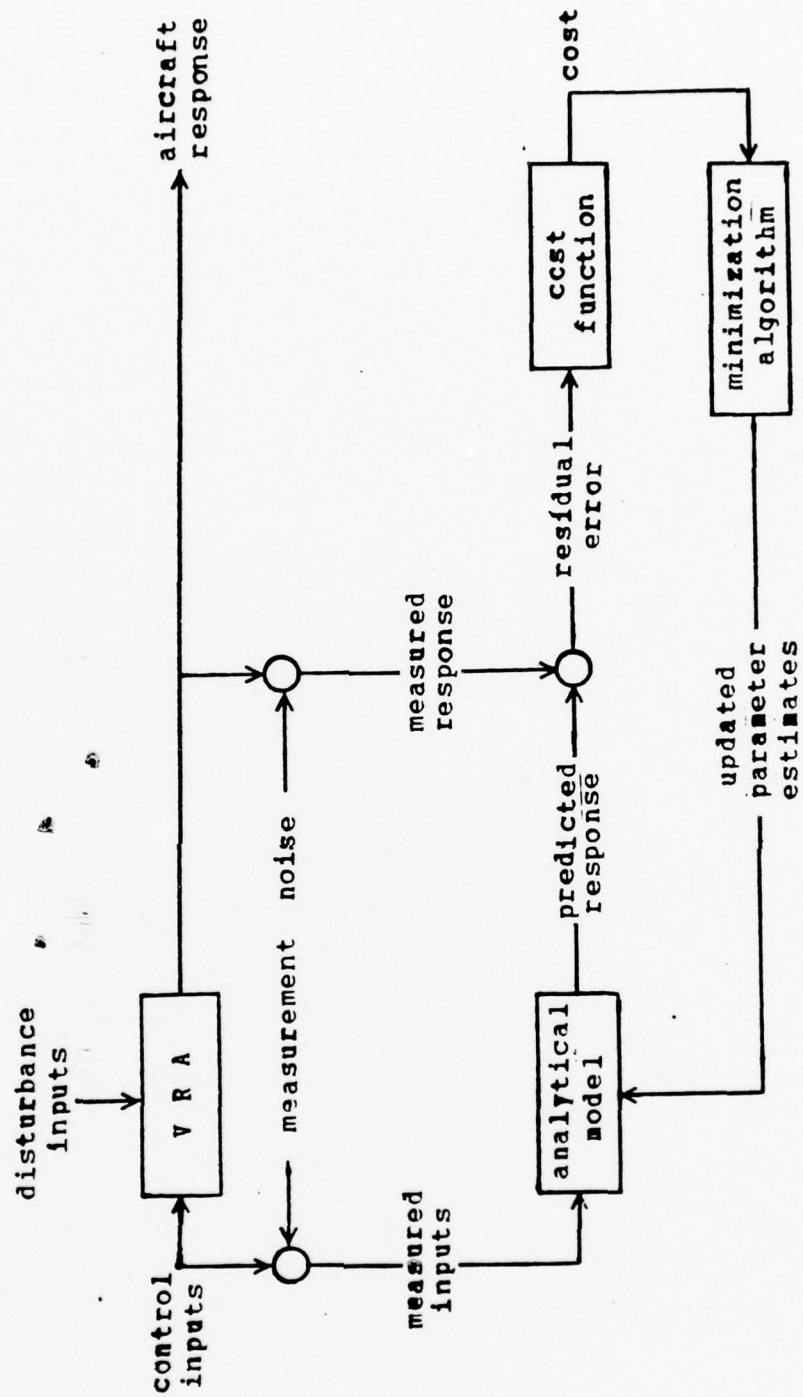
FIGURE 1. BLOCK DIAGRAM OF THE PARAMETER ESTIMATION PROCESS.

2 - 2

these factors is discussed below.   :   .

2.1 Equations_of_Motion

Beginning with 12 state variables, a nonlinear, time-varying, 6-degree-of-freedom model describes the motion of an aircraft in an inertial reference frame. The earth is assumed to be fixed in space, and earth curvature is neglected. Variations in atmospheric properties and gravity with altitude and position perturbations of interest also are assumed negligible. Aircraft mass, and mass distribution are assumed constant, and the aircraft is assumed to be a rigid body, leading to the nonlinear differential equation:

$$\underline{\dot{x}}(t) = \underline{f}(\underline{c}, \underline{x}, \underline{u}, \underline{w}) \tag{1}$$

where $\underline{f}$ is a vector of specific forces, moments and kinematic effects, $\underline{c}$ is a vector of aircraft parameters to be identified, $\underline{x}$ is the state vector, $\underline{u}$ is the control vector, and $\underline{w}$ is the disturbance vector.

Assuming, in addition, that the aircraft is in steady equilibrium at its nominal flight condition implies that the

2 - 3

equations of motion are time invariant. The 6 dynamic equations are converted from the inertial-axis system to the body-axis system using inertial-to-body-axis transformation matrices from Ref 5. Stochastic inputs , $\underline{v}$, to the model are assumed negligible.

The equations are linearized by Taylor series expansion, taking only the perturbation solutions. The 4 state variables representing "pure" integrals of other variables, (x y z ψ) are dropped next, since they add little information to the model. Products and squares of perturbation quantities are assumed negligible. Sines and cosines of perturbation angles are assumed to be approximately the angles and one, respectively. The linear differential equation model derived from Eq 1 then can be expressed as

$$\dot{\underline{x}} = \begin{bmatrix} a1 & a2 \\ a3 & a4 \end{bmatrix} \underline{x} + \begin{bmatrix} b1 \\ b2 \end{bmatrix} \underline{u} \qquad (2)$$

where a1 and b1 are longitudinal mode derivative matrices, a4 and b2 are lateral-directional mode derivative matrices, and, a2 and a3 are mode coupling derivative matrices.

$$\underline{x} = [u \; w \; q \; \theta \; v \; p \; r \; \phi]^T \qquad (3)$$

2 - 4

$$\underline{u} = |~\delta e~~\delta a~~\delta r~~\delta sf~~1~|^{T} \tag{4}$$

Inertial cross-products between the longitudinal and lateral axes and the lateral and normal axes are assumed to be negligible ($I_{XY} = I_{YZ} = 0$). Straight and level, trimmed flight further simplifies the equations, since

$$\beta = p = q = r = \phi = 0 \tag{5}$$

The translational states are converted to more easily measurable angles by the relationships:

$$w~/~(u^2 + v^2 + w^2)^{1/2} = \sin \alpha$$

$$u~/~(u^2 + v^2 + w^2)^{1/2} = \cos \alpha \tag{6}$$

$$v~/~(u^2 + v^2 + w^2)^{1/2} = \sin \beta$$

Figure 2 defines the body-axis-measurable aircraft states and control deflections in their positive sense, used in the equations of motion. The following body-axis, linear, time-invariant, perturbation differential equations are uncoupled into a longitudinal motion set and a lateral-

2 - 5
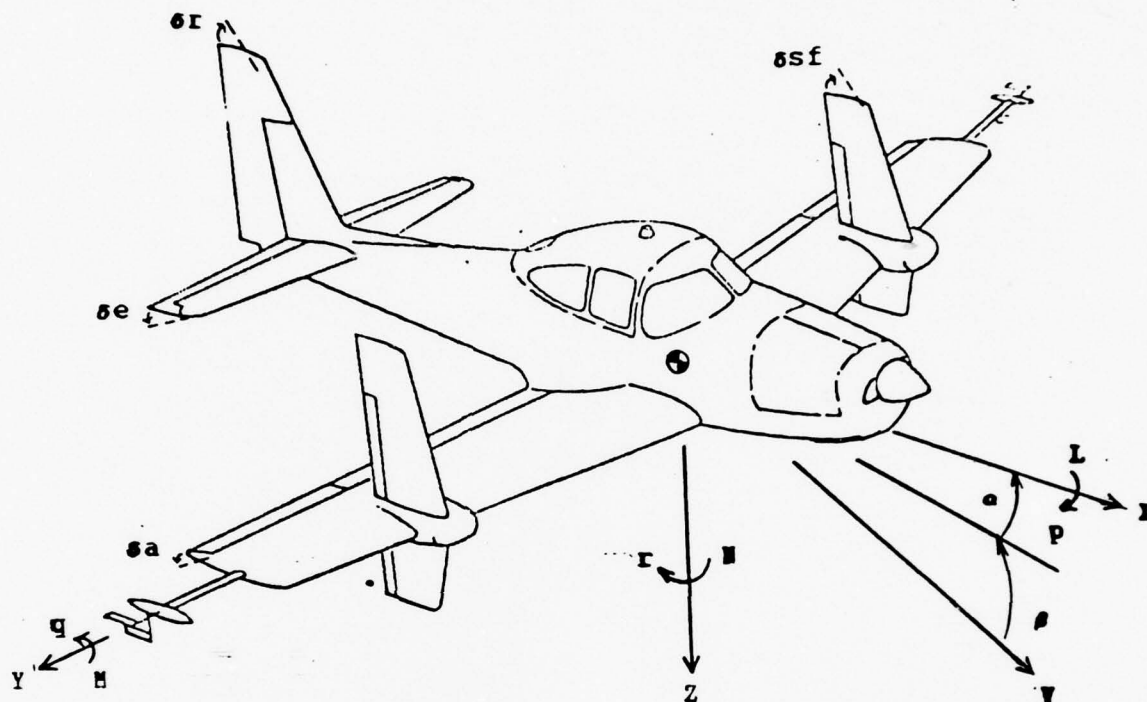
FIGURE 2. SYSTEM OF BODY AXES SHOWING POSITIVE SENSE OF
ANGLES, FORCES, AND MOMENTS.

2 - 6

directional set:

$$\dot{\underline{x}} = A\,\underline{x} + B\,\underline{u} \tag{7}$$

$$
A =
\begin{bmatrix}
X_V & X_\alpha & X_q - \sin\alpha & -g/V\,\cos\theta \\
Z_V & Z_\alpha & Z_q + \cos\alpha & -g/V\,\sin\theta \\
M_V & M_\alpha & M_q & 0 \\
0 & 0 & 1 & 0
\end{bmatrix}
\tag{8}
$$

$$\underline{x} = \begin{bmatrix} V & \alpha & q & \theta \end{bmatrix}^T \tag{9}$$

$$
B =
\begin{bmatrix}
X_{\delta e} & X_o \\
Z_{\delta e} & Z_o \\
M_{\delta e} & M_o \\
0 & \dot{\theta}_o
\end{bmatrix}
\tag{10}
$$

2 - 7

$$\underline{u} = \begin{bmatrix} \delta e & 1 \end{bmatrix}^T \tag{11}$$

For the lateral-directional case:

$$A = \begin{bmatrix} Y_\beta & Y_p + \sin\alpha & Y_r - \cos\alpha & g/V\cos\phi \\ L_\beta & L_p & L_r & 0 \\ N_\beta & N_p & N_r & 0 \\ 0 & 1 & \cos\phi\tan\theta & 0 \end{bmatrix} \tag{12}$$

$$\underline{x} = \begin{bmatrix} \beta & p & r & \phi \end{bmatrix}^T \tag{13}$$

$$B = \begin{bmatrix} Y_{\delta a} & Y_{\delta r} & Y_{\delta sf} & 0 \\ L_{\delta a} & L_{\delta r} & L_{\delta sf} & L_0 \\ N_{\delta a} & N_{\delta r} & N_{\delta sf} & N_0 \\ 0 & 0 & 0 & \dot{\phi}_0 \end{bmatrix} \tag{14}$$

2 - 8

$$\underline{u} = [\ \delta a\ \ \delta r\ \ \delta sf\ \ 1\ ]^T \tag{15}$$

where A is the fundamental matrix, and B is the control effect matrix. Dividing the equations into two sets still allows determination of parameters coupling the two sets as suggested in Ref 6. The division reduces computation time, model complexity and order, simplifies input design, and is common practice.

Inclusion of certain unsteady aerodynamic parameters, such as $M_{\dot{\alpha}}$, is accomplished using the acceleration transformation matrix, R, in the dynamic equations:

$$R\ \underline{\dot{x}} = A\ \underline{x} + B\ \underline{u} \tag{16}$$

The R matrix is the identity matrix minus the matrix of unsteady aerodynamic parameters.

The aircraft analytical model is made up of three sets of linear equations. The dynamic equations or equations of motion (17) were just derived. The output equations (18) define the observation relationship of states and state rates. The observation equations (19) incorporate outputs and measurement noise. Modeling errors and instrument

2 - 9

biases are assumed negligible.

$$\dot{\underline{x}} = A \, \underline{x} + B \, \underline{u} \qquad\qquad (17)$$

$$\underline{y} = G \, \underline{x} + H \, \underline{u} \qquad\qquad (18)$$

$$\underline{z} = \underline{y} + \underline{n} \qquad\qquad (19)$$

The G and H matrices incorporate the A and B matrices and the identity matrix to produce states and state rates in the output vector. $\underline{n}$ is the measurement noise vector. Measurement noise is assumed to be a stationary, Gaussian, white noise process. Control measurement noise is assumed to be negligible.

In summary , the following assumptions are observed in the aircraft analytical model:

. Turbulence, modeling errors, and instrument biases are negligible.

. Airframe is a rigid body; i.e., there are no significant structural or aeroelastic modes.

. Earth is fixed in space.

. Mass and mass distribution of the aircraft are constant.

. Products and squares of perturbation quantities are assumed negligible.

2 -10

. Variations in atmospheric properties with altitude perturbations of interest are negligible.

. Trim values are $\beta = p = r = q = \phi = 0$

. The inertia cross-products I_{XY} and I_{YZ} are negligible.

. Measurement noise is a stationary, Gaussian, white noise process.

. No stochastic inputs are allowed. Control measurement noise is negligible.

2.2 Cost Function

The objective of maximum likelihood estimation is to maximize the probability density function, $p(\underline{c}|Z_N)$, of the unknown parameters, $\underline{c}$, (stability and control derivatives, state initial conditions, aerodynamic biases) conditioned on the state and control measurements, Z_N. In other words, the estimator must maximize the likelihood that an estimate of the unknown stability and control derivatives in the equations of motion will produce the measured state time histories. Bayes's rule expresses this conditional probability density function in terms of more readily computed quantities:

2 -11

$$p(\underline{c}|Z_N) = p(Z_N|\underline{c}) \ p(\underline{c}) \ / \ p(Z_N) \qquad (20)$$

where $p(Z_N|\underline{c})$ is the probability density of the measurements conditioned on the unknown parameters, $p(\underline{c})$ is the prior probability density of the parameters, and $p(Z_N)$ is the probability of the measurements and equals 1.

A sequential computation of $p(\underline{c}|Z_N)$ can be derived from Bayes's rule. $p(\underline{c})$ is approximated by $p(\underline{c}|Z_{N-1})$, the probability density of the parameters conditioned on N-1 sample time measurements, and each prior conditional probability density function is defined in a like manner, back to the starting point of the data. Then,

$$p(\underline{c}|Z_N) = \prod_{i=1}^{N} p(Z_N|\underline{c}) \ p(\underline{c}|0) \qquad (21)$$

where $p(\underline{c}|0)$ is the probability density of the parameters prior to any measurements.

If measurement errors, process errors, and state initial conditions have stationary, Gaussian probability distributions, then the probability distribution of the parameters conditioned on the measurements will also be Gaussian. In addition, the probability density of the measurements conditioned on the parameters is the same as

2 -12

the probability density of the measurements conditioned on the residual calculated using the parameters (Ref 7):

$$p(\underline{z}_i | \underline{y}_i) = \frac{1}{(2\pi)^{N/2} |D1^{-1}|^{1/2}} \; exp\left[-\frac{1}{2}(\underline{z}_i - \underline{y}_i)^T D1 (\underline{z}_i - \underline{y}_i)\right]$$

(22)

where D1 is the measurement error covariance matrix, and $\underline{z}$ is the observation vector at sampling time i. Taking advantage of the properties of logarithms, the log likelihood function is:

$$\ln p(\underline{c} | \underline{z}_N) = -\frac{1}{2} \sum_{i=1}^{N} (\underline{z}_i - \underline{y}_i)^T D1 (\underline{z}_i - \underline{y}_i)$$

$$-\frac{1}{2} \sum_{i=1}^{N} \ln (2\pi)^{N/2} |D1^{-1}|^{1/2}$$

$$-\ln p(\underline{c} | 0)$$

(23)

For a constant error covariance matrix and a constant estimate of the probability density of the parameters prior to any measurements, the quadratic cost function, J, which neglects the latter two terms is minimized when the log likelihood function is maximized:

2 -13

$$J = \frac{1}{N-1} \sum_{i-1}^{N} (\underline{z}_i - \underline{y}_i)^T D1 (\underline{z}_i - \underline{y}_i)$$

<div align="right">(24)</div>

where N is the number of sampling instants, i is the sampling index, and D1 is the measurement error weighting matrix (ideally it is the inverse of the error covariance matrix).

This mean-squared-error criterion serves many useful ends. The cost function, J, compares predicted aircraft motion with measured flight time histories. It reflects the confidence in the measurement of those time histories. It weighs large errors more heavily than small errors, and it is simple to use.

There are several ways of determining the D1 weighting matrix. One approach is to base the weighting on published statistical properties of the instrument noise. Reference 7 employs a Kalman Filter state estimator to estimate the measurement error covariance matrix, then inverts it to form the equivalent of D1. Reference 3 and 8 suggest using the smallest mean-squared-error obtainable from the test flight data as a measure of the noise in a measured variable.

In this study, D1 matrix elements were determined following the recommendations in Ref 8. The diagonal elements of D1 first were estimated from published

instrument accuracy and resolution information. Next, the cost function was minimized with the initial D1 matrix. Elements of the D1 diagonal were replaced by one over the mean-squared-error in a state variable if the weighted mean squared-error was not approximately equal to one:

$$d_{ii} = 1 / \sigma_{ii}^2 \qquad\qquad i = 1,\ldots,l \qquad (25)$$

where l is the number of elements in the observation vector, $\underline{z}$. This process was repeated with the updated D1 matrix until all diagonal D1 elements resulted in weighted mean squared-errors near one. All off-diagonal D1 elements were set to zero since correlation in instrument noise was assumed to be small.

The cost function was modified to consider à priori estimates of the parameters in the cost function:

$$J = \frac{1}{N-1} \sum_{i-1}^{N} (\underline{z}_i - \underline{y}_i)^T D1 (\underline{z}_i - \underline{y}_i)$$

$$+ (\underline{c} - \underline{c}_o)^T K D2 (\underline{c} - \underline{c}_o) \qquad (26)$$

where $\underline{c}$ is a vector of all parameters to be identified, $\underline{c}_o$ is the vector with à priori values of the parameters to be

2 -15

identified, D2 is a symmetric weighting matrix reflecting the relative confidence in à priori estimates, and K is a constant reflecting the importance of a departure from à priori values over estimation from flight data.

À priori weighting permits the use of additional information in the estimation process. Reference 9 suggests that the use of à priori weighting prevents estimates from changing from à priori values unless there is sufficient information in the flight data to justify a change. Reference 7 discusses advantages in numerical computations through the use of à priori weighting. The cost function, J, as defined in Eg 26 forms the basis of the Modified Maximum Likelihood Estimation algorithm which is used here.

2.3 Modified Newton-Raphson Minimization Algorithm

Reference 8 describes several parameter identification methods and their associated cost functions. The advantages of using digital computation to reduce the cost function are also described. Digital computation more readily analyses large amounts of data with little or no operator judgement required. The Modified Newton-Raphson minimization algorithm approximates the first and second gradients of the

cost function with respect to the unknown parameters, and from these, it estimates the increments in the parameters which drive the cost function to a minimum.

The Newton-Raphson iteration technique finds a zero of a nonlinear function of several parameters (Ref 4). Setting the gradient of the cost function to zero defines the minimum cost set of parameters. Therefore, the Newton-Raphson technique can be used to derive a minimization algorithm.

The gradient of the cost function can be expanded in Taylor's series about the kth iteration value of $\underline{c}$:

$$(\nabla_c J)_{k+1} = (\nabla_c J)_k + (\nabla_c^2 J)_k (\underline{c}_{k+1} - \underline{c}_k) \qquad (27)$$

$$+ \text{ Higher Order Terms}$$

where $(\nabla_c J)_k$ is the first gradient of the cost function with respect to the parameters at the kth iteration, and $(\nabla_c^2 J)_k$ is the second gradient of the cost function. Neglecting higher order terms, the increment of the parameters that makes $(\nabla_c J)_{k+1}$ approximately equal to zero is:

2 -17

$$(\underline{c}_{k+1} - \underline{c}_k) = -\left[(\nabla_c^2 J)_k\right]^{-1} (\nabla_c J)_k \tag{28}$$

This is the familiar form of the Newton-Raphson algorithm. The first and second gradients of the cost function are defined in terms of the gradients of the residual:

$$(\nabla_c J)_k = \frac{2}{N-1} \sum_{i=1}^{N} (\underline{z}_i - \underline{y}_{ik})^T D1 \, \nabla_c (\underline{z}_i - \underline{y}_{ik}) \tag{29}$$

$$(\nabla_c^2 J)_k = \frac{2}{N-1} \sum_{i=1}^{N} \nabla_c (\underline{z}_i - \underline{y}_{ik})^T D1 \, \nabla_c (\underline{z}_i - \underline{y}_{ik}) \tag{30}$$

$$+ \frac{2}{N-1} \sum_{i=1}^{N} (\underline{z}_i - \underline{y}_{ik})^T D1 \, \nabla_c^2 (\underline{z}_i - \underline{y}_{ik})$$

with

$$(\underline{z} - \underline{y})_k = (\underline{z} - \underline{y})_{k-1} + \nabla_c (\underline{z} - \underline{y}) (\underline{c}_k - \underline{c}_{k+1}) \tag{31}$$

where $\nabla_c (\underline{z}_i - \underline{y}_{ik})$ is the first gradient of the residual for the kth iteration and the ith sampling instant, and $\nabla_c^2 (\underline{z}_i - \underline{y}_{ik})$ is the second gradient of the residual for the kth iteration and the ith sampling instant.

Calculation of the first gradient of the residual is straightforward (Ref 8) and is analogous to the calculation of the "sensitivity equations" in Ref 10:

2 -18

$$\nabla_c (\underline{z} - \underline{y}) = -(\nabla_c G)\underline{x} - G(\nabla_c \underline{x}) - (\nabla_c H)\underline{u} - H(\nabla_c \underline{u})$$

$$(32)$$

Balakrishnan shows in Ref 11 that the second gradient of the residual goes to zero as the parameter estimates approach their true values. Neglecting this term reduces the amount of computation required, and still results in asymptotically unbiased estimates. The algorithm is now referred to as the Modified Newton-Raphson algorithm.

Reference 8 discusses the use of an approximation to the Cramèr-Rao bound in conjunction with the Modified Newton-Raphson minimization algorithm used here to indicate confidence levels for the parameter estimates. If the actual parameter covariance matrix were known, it would indicate which parameters had been most reliably estimated. Reference 11 shows that this covariance matrix is bounded from below by the matrix Cramèr-Rao bound. By assuming that the estimates obtained using the Modified Newton-Raphson algorithm are asymptotically unbiased and that the measurement noise, $\underline{n}$, is a stationary, Gaussian, white noise process, the matrix Cramèr-Rao bound is the inverse to the second gradient of the cost function matrix with respect to the parameters. Similar assumptions are used in Ref 10 to

2 -19

obtain an approximation to the parameter covariance matrix. The Cramèr-Rao lower bounds to the standard deviations in the parameter estimates are used in this thesis to indicate the confidence in estimates from different sets of time histories.

Reference 4 is a listing of a program written in FORTRAN IV using the equations of motion, cost function, and minimization algorithm here described. Authored by Maine and Iliff, it has been used to analyze thousands of maneuvers on several aircraft.

This program generates state time history estimates using the state transition matrix defined in Ref 12:

$$\underline{x}(t_2) = \Phi \, \underline{x}(t_1) + \int \Phi(t_1, \tau) \, B \, \underline{u}(\tau) \, d\tau \tag{33}$$

where Φ is the state transition matrix and $\underline{u}$ is the measured control vector.

Normal and lateral acceleration time history estimates are made using Eq 18. The specific equations are restated here:

$$a_n = -\frac{V}{g} Z_\alpha \, \alpha - \frac{V}{g} Z_{\delta e} \, \delta e - \frac{V}{g} Z_o + \cos\phi \, \cos\theta \tag{34}$$

$$a_y = \frac{V}{g} Y_\beta \beta + \frac{V}{g} Y_{\delta a} \delta a + \frac{V}{g} Y_{\delta r} \delta r + \frac{V}{g} Y_{\delta sf} \delta sf + \frac{V}{g} Y_o \tag{35}$$

Control measurement noise is assumed to be negligible. The validity of this assumption is evident in the quality of the parameter estimates.

This program was used with only minor modification on VRA flight data collected from two test flights. The next chapter describes the collection and processing of that data and the preliminary inputs to the computer program.

3. DATA ACQUISITION AND PRELIMINARY INPUTS FOR PARAMETER ESTIMATION

Princeton's VRA has a full complement of instruments and necessary telemetry to measure all states and some state rates of interest. Upon calibrating this instrument package, flight data were collected and recorded for processing. Analog-to-digital conversion, application of calibrations, and correction of time shifts prepared the raw data for use in the estimation program. In addition, true airspeed and dynamic pressure were calculated, and time histories were selected.

Specifying aircraft dimensions allowed nondimensionalization of derivatives for comparison with published values. The measurement error weighting matrix was approximated using several time histories. Preliminary estimates of the unknown parameters were taken from unpublished analog matching results and published estimates.

3.1 Instrumentation

In the aircraft, instrument readings and control surface positions are sampled at twenty and forty samples

per second (SPS) with a fixed time delay between measurements. The data are telemetered to a ground station as a frequency-modulated, single channel, pulse duration signal where it was recorded on tape. The pulse duration contains the information. Table 1 lists the states and controls measured on Flights 1 and 2.

TABLE 1. MEASURED STATES AND CONTROLS OF FLIGHTS 1 AND 2.

	Flight 1	Flight 2
α	X	X
q	X	X
V	X	X
θ	X	X
a_n		X
δe	X	X
β	X	X
p	X	
r	X	X
ϕ	X	X
a_y	X	X
δa	X	X
δr	X	X
δsf	X	X

The VRA has two angle-of-attack vanes, one mounted on a boom extending from each wing, at the quarter chord. This position does not require an angular rate correction, but previous test flights indicate that an aerodynamic scale factor of 1.6 must be used to correct for upwash effects. The signals of the two vanes are averaged prior to transmission via telemetry.

Perturbations in the wing vortex flow with changing angle-of-attack and aileron deflection caused a dynamic error in the single sideslip angle vane mounted on the right wing boom. In Figure 3, the positive sideslip angle perturbation (M) of approximately 1 deg at 1 sec is nearly in phase with the aileron pulse input. The sideslip angle estimate (E) based on present study stability and control derivatives does not predict the measured perturbation. Examination of the lateral acceleration measurement shows some acceleration due to aileron deflection but it is questionable whether the magnitudes of the perturbations are in agreement. Since the aileron pulse time histories came from the first test flight, side-force derivative estimates using those time histories are suspect. After the first flight an additional vane was added to the left wing boom, and both signals then were averaged prior to telemetry
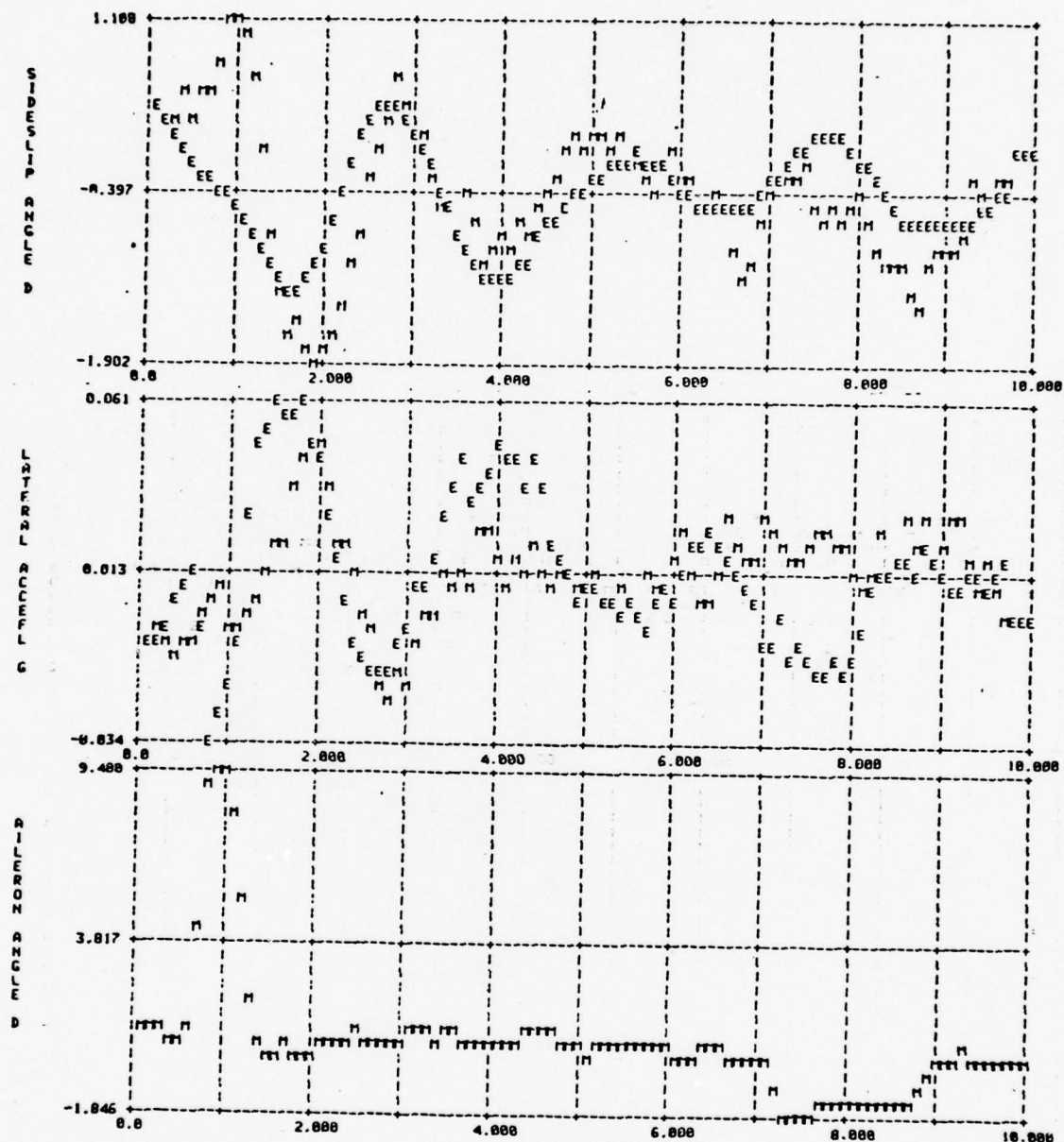
FIGURE 3. COMPARISON OF SIDESLIP ANGLE AND LATERAL ACCELERATION MEASUREMENTS (M) FOR A FLIGHT 1 AILERON INPUT TIME HISTORY (E- STATE ESTIMATES BASED ON PRESENT STUDY STABILITY AND CONTROL DERIVATIVES). (ABSCISSA IS TIME IN SEC)

3 - 4

transmission. This correction must be evaluated. An angular rate correction for the vanes' 1.3 ft displacement above c.g. is employed.

The attitude gyros, pitch rate gyros, and normal and lateral accelerometers are clustered about the main wing spar, on or near the c.g. This location reduces the sensitivity of the pitch rate gyro to structural vibration. On Flight 1, a single accelerometer was available and it measured lateral accelerations. A second accelerometer was installed prior to Flight 2. Figure 4 shows a typical lateral acceleration time history from Flight 2. The .25 g noise band in the measurement (M) is not apparent for the Flight 1 lateral acceleration time history in Figure 3. Since the lateral acceleration measurement was not useful, the quality in the Dutch roll related stability and control derivatives was degraded. Further investigation into the causes of this noise are required.

The roll and yaw rate gyros are mounted in the equipment bay behind the c.g. The poor lateral acceleration signal and the failure of the roll rate gyro degraded the estimation of side-force and rolling moment derivatives from Flight 2 data. Estimation of lateral derivatives still was attempted since sideslip angle and bank angle time histories

3 - 5
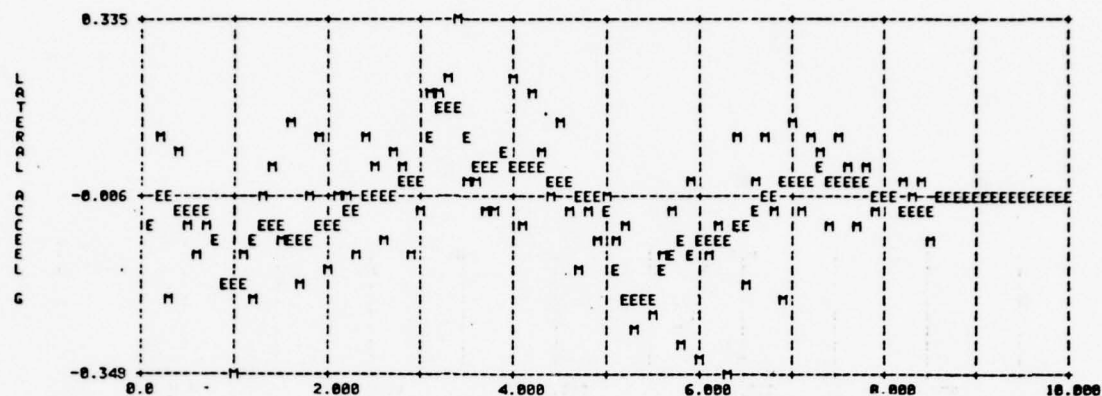
FIGURE 4. NOISY LATERAL ACCELERATION MEASUREMENT (M) FROM FLIGHT 2 SIDE-FORCE INPUT TIME HISTORY (E- STATE ESTIMATES BASED ON PRESENT STUDY STABILITY AND CONTROL DERIVATIVES). (ABSCISSA IS TIME IN SEC)

were available.

The aircraft pitot boom is mounted below and forward of the right wing. The two static ports are on either side of the fuselage. Large pitch rates accompanying elevator doublets produced a noticeable instrument response in the velocity measurement as seen in Figure 5. The large velocity perturbation starting at 2-sec corresponds to a .2 g deceleration that was not confirmed by the pilot. This dynamic velocity error is produced by the changing pressure

3 - 6
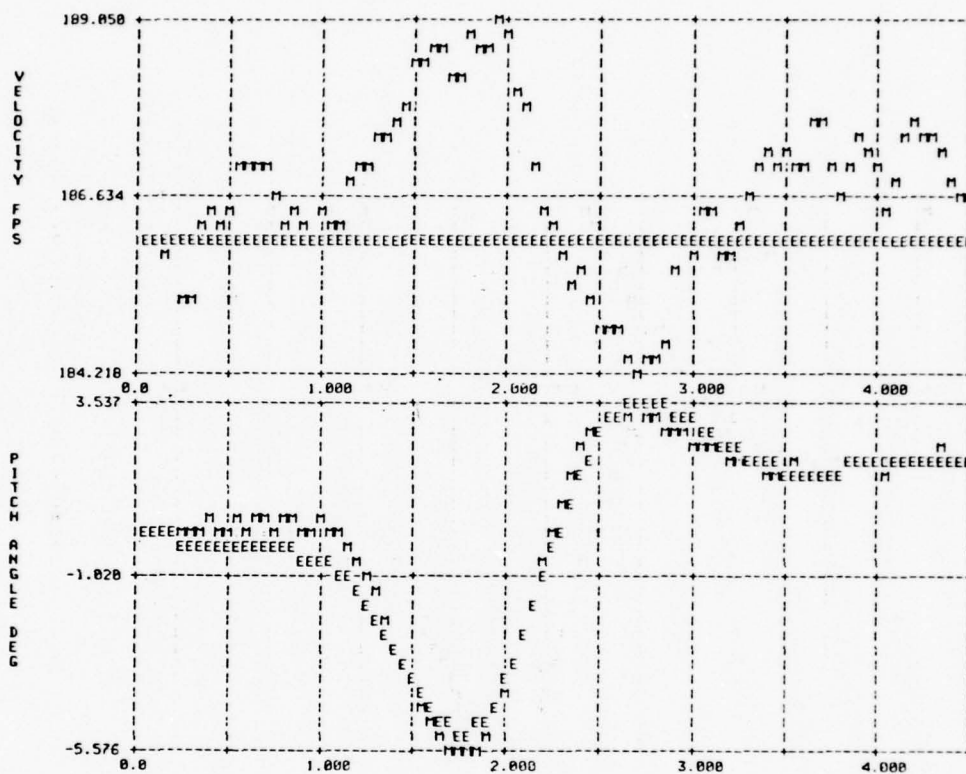
FIGURE 5. DYNAMIC VELOCITY MEASUREMENT ERROR (M) FOR A FLIGHT 2 ELEVATOR INPUT TIME HISTORY (E- STATE ESTIMATES BASED ON PRESENT STUDY STABILITY AND CONTROL DERIVATIVES).

3 - 7

measured by the static port with rapid changes in flow over the wing. Although this problem is not a serious concern to production models of the Navion, the dynamic error prevented use of the velocity time history in estimating longitudinal derivatives from elevator doublets.

3.2 Calibration

Aircraft instruments and telemetry signals were calibrated prior to each flight. Deflecting the instruments and control surfaces to measured positions or rates, the telemetry signals were recorded in units of percent telemetry. These units correspond to the percentage of the maximum pulse duration transmitted via telemetry. Scale and bias factors were calculated for each instrument and control surface using linear regression. Table 2 lists signal scale and bias factors for Flights 1 and 2. The angle-of-attack factors reflect corrections for upwash effects.

Overall, there is little change in scale factors and biases between the two flights, a surprising result considering that the instruments were replaced during the 3-month period between flights, that there was normal wear and tear of the data acquisition system with usage, and that

a number of people were involved in making the calibrations.

The bias differences for the angle-of-attack and sideslip vanes were expected due to differences in alignment procedure. The vanes were faired with the wing for the zero reference values prior to Flight 1, and they aligned to produce 17 "units" on the angle-of-attack meter and zero "units" on the sideslip meter as zero reference values prior to Flight 2.

The scale factor and bias differences for the bank angle attitude gyro are of concern. Only 4 data points were used to calculate the scale factor and bias for the first test flight, and it is possible that 2 data points were beyond the linear range of the ground station. Since the response of the attitude gyro for Flight 2 was not similar to the data for Flight 1, it was not felt that using the scale factor and bias from Flight 2 was superior to using questionable values from Flight 1. Comparison of roll rate and roll angle time histories for Flight 1 did not point to any gross discrepancies.

The lateral accelerometer values represent two different accelerometers, telemetered on two different channels. In light of the fact that the lateral acceleration time histories for Flight 2 are very noisy,

3 - 9

TABLE 2. CALIBRATION SCALE FACTORS AND BIASES FOR
FLIGHTS 1 AND 2.

	Scale Factor			Bias		
	Flt. 1	Flt. 2	Percent Change	Flt. 1	Flt. 2	Percent Change
α	-.1362	-.1315	2	8.30	5.88	17
q	-.4725	-.4892	2	20.77	22.19	3
V	-.7031	------	-	129.79	------	-
θ	-.3877	-.3917	1	19.30	20.43	3
a_n	------	.0153	-	------	-.7970	-
β	-.4385	-.4301	1	20.85	17.49	9
p	-.5318	-.5473	1	24.34	24.34	2
r	.4290	.4399	1	-19.38	-20.45	3
ϕ	.75777	.8934	8	-37.36	-40.87	4
a_y	.0170	.0176	2	-.7273	-.8196	6
δe	-1.0220	-.9150	5	38.11	31.99	9
δa	-.5295	-.4862	4	23.29	21.24	5
δr	.3750	.4396	8	-19.19	-25.76	15
δsf	-.8101	-.7991	1	43.50	44.42	1

pointing to some installation error or hardware problem, it
is surprising that these terms are as close as they are.

The relatively large difference in control surface

3 -10

scale factors and biases between flights was not expected. No new potentiometers and no extensive rewiring occurred between flights. Since the state and state rate factors changed little, it is unlikely that the telemetry package or the ground station produced the differences. The side-force surface calibrations used protractor markings permanently etched on the wing which would tend to reduce human error in measurement. The elevator and aileron deflection angles were measured using hand-held bubble protractors, and the rudder measurements for Flight 1 were made using a damaged protractor. Human error in measuring surface deflections might be reduced by using protractors specially constructed for each surface and bolted in place during calibrations. Such a protractor has already been constructed and is now used for the rudder deflection measurements. The ease of using this protractor suggests that human error is being reduced.

3.3 Data Collection

The data used in this study were obtained from two test flights of the VRA at 105 KIAS. Outside air temperature and pressure altitude were noted for later use in calculating

3 -11

true airspeed and dynamic pressure. The applied control inputs included elevator doublets and pulses, aileron pulses, rudder doublets, and side-force surface pulses and doublets.

During Flight 2, aircraft pitch angle and angle-of-attack were measured using a bubble protractor and angle-of-attack meter. Both indicated a zero pitch angle and angle-of-attack (within 1/2 deg) with respect to the fuselage reference line for straight-and-level flight at 105 KIAS.

The aircraft nominal altitude was selected during flight to minimize turbulence. 105 KIAS was the flight airspeed used for two other research programs conducted concurrently with this study. It guarantees low trim angle-of-attack to remain within the linear range of the lift curve slope during control inputs. In addition, the control surfaces are more effective than at slower speeds, thus producing state perturbations with good signal-to-noise ratios (Ref 13). The quality of the control inputs reflects the experience of the test pilot with analog matching parameter estimation.

The VRA is now equipped with a Microprocessor Digital Flight Control System that has demonstrated its ability to

3 -12

produce precise square elevator pulses. For future parameter estimation studies, this system could be used to input precise control deflections better suited to excite several aircraft modes of motion simultaneously or sequentially (Ref 14). In addition optimal input design studies could be demonstrated using the VRA (Ref 3,16).

3.4 Analog-to-Digital Conversion

Flight test data were recorded during flight on a Honeywell 7600 1-inch tape recorder. Due to equipment compatibility requirements the data were re-recorded on 1/4-inch tape. The tape was transferred to another facility to be digitized. The discrete analog signals on the tape were converted to "boxcar" analog signals using integrator circuits in the ground station (Ref 16). The signals were sampled simultaneously at 40 SPS per signal and digitized by a SEL 600 Analog-to-Digital Converter. The digitized samples were recorded in 6-bit BCD on 7 track, 1600 bit-per-inch magnetic tape using an AMPEX Digital Recorder.

The resulting tape cannot be processed directly by a FORTRAN program because FORTRAN does not recognize the manner in which signs of samples are stored on the tape.

The "Seven to Nine Track Tape Conversion Program", written by Richard B. Gilbert, Technical Staff Member in the Department of Mechanical and Aerospace Engineering, reads the tape, scales the data to percent telemetry and records it in an acceptable FORTRAN format.

This analog-to-digital conversion procedure is time consuming and it adds several sources of errors in the raw data. Each step in the process was delayed by failures in aging equipment. Plans are being made to replace this equipment. The replacement system should digitize the discrete analog samples directly from the original data tape. This would prevent the addition of noise to the data by the additional tape recorders and the ground station. It also would eliminate the ground station as a source of bias errors.

3.5 Data Scaling

After producing a magnetic tape containing digitized flight time histories in an acceptable FORTRAN format the data must be converted into engineering units, interpolated to reduce the errors produced by time shifts, and corrected for compressibility and density effects. This final data

processing was performed using a FORTRAN program entitled 'Scaling', written as part of this research. The program first applies the calibration scale factors and biases to convert the digitized data from percent telemetry to engineering units.

Scaling calculates true airspeed and dynamic pressure from measured indicated airspeed and pilot judged nominal pressure altitude and outside air temperature. The equations used in these calculations were derived from the perfect gas law and definitions of the standard atmosphere. They are taken directly from Ref 17:

$$V_{true} = 147 \sqrt{(Ta+273.16)\left\{\left[\frac{\left[1 + 1.6\times10^{-7} \times V_c^2\right]^{7/2} - 1}{(1 - 6.88\times10^{-6} H_c)^{5.2561}} - 1\right]^{2/7} - 1\right\}}$$

(36)

$$\bar{q} = \frac{1}{2} \rho V_{true}^2$$

(37)

where Ta is absolute air temperature(deg K), V_c is calibrated airspeed, H_c is calibrated pressure altitude, and, ρ is air density and equals atmospheric pressure divided by Ta and 3090.

3 -15

Reference 18 discusses the effects of time delays between sampling instants of states and controls on the performance of a maximum likelihood estimator. Steers and Iliff concluded that delays of control measurements caused the greatest degradation in the accuracy of estimates. Since no measured quantities were sampled simultaneously prior to transmission to the ground, and control measurements lagged state measurements by as much as 30 percent of the sampling period, it was deemed important to interpolate between sampling instants to produce data with negligible time shifts. Scaling also performs this interpolation on a measurement, s, using the following equation:

$$\bar{s}_i = s_i + k(s_{i+1} - s_i) \tag{38}$$

where $k = 1 - \text{time delay/sampling period}$ (39)

The analog-to-digital converter samples all quantities simultaneously and therefore does not add additional delays. Since sideslip angle is the first sampled signal, all data were interpolated to the time corresponding to the sideslip angle sampling instant.

3 - 16

Finally, Scaling calculates means and standard
deviations of all states, state rates, and controls measured
as an aid in determining biases. These biases reflect fixed
biases used by the ground station and analog-to-digital
converter in manipulating the data, fixed instrument biases
in flight (for example, the trim angle-of-attack vane
position is fixed by flow over the wing in trimmed flight),
and instrument drift between calibration of the instruments
and recording of the data. Fixed biases in states, state
rates, and controls are inputs to the Modified Maximum
Likelihood Estimation program.

3.6 Inputs To The Estimation Program

Time histories to be used in the estimation program
were selected primarily by two criteria. First, the time
history had to be free of dropouts and other equipment
produced anomalies as discussed in Ref 9. Second, control
inputs were chosen that appeared to be greater than 5 times
the noise band (peak to peak) of the control measurement to
insure a good signal-to-noise ratio (ratio of largest signal
perturbation to noise band).

Table 3 lists aircraft dimensions and flight conditions

3 -17

TABLE 3. AIRCRAFT DIMENSIONS AND FLIGHT CONDITIONS.

```
Wing:
      Area                                 180.0   FT²
      Span                                  33.38  FT
      Chord                                  5.67  FT
      Leading Edge Sweep                     3.0   DEG
      Dihedral                               7.5   DEG
      Root Incidence                         2.0   DEG
      Tip Incidence                         -1.0   DEG
      Airfoil:
            Tip                        NACA 6410R
            Root                       NACA 4415R
      Aileron:
            Area                             5.4   FT²
            Deflection                   ± 20.0    DEG
      Flap:
            Area                            83.6   FT²
            Deflection                   ± 30.0    DEG
      Horizontal Tail:
            Area                            43.0   FT²
            Incidence                       -3.0   DEG
            Airfoil                    NACA 0012
      Elevator:
            Area                            14.1   FT²
            Deflection         UP 30,DOWN 20       DEG
Vertical Tail:
      Area                                  18.1   FT²
      Airfoil                    MODIFIED NACA 0013.2
      Fin Offset                             2.0   DEG
      Rudder:
            Area                            11.6   FT²
            Deflection        LEFT 23,RIGHT 17     DEG
Side Force Surface:
      Area                                  16.0   FT²
      Airfoil                    NACA 0012
      Deflection                         ± 30.0    DEG
Gross Weight                             2609.0    LB
I                                        1573.7 SLUG-FT²
 X
I                                        2736.0 SLUG-FT²
 Y
I                                        3673.8 SLUG-FT²
 Z
```

TABLE 3. (CONTINUED).

	Flight 1	Flight 2
Pressure Altitude	3500 FT	6500 FT
Nominal Indicated Airspeed	105 KT	105 KT
Outside Air Temperature	0 degC	10 degC
Flap Setting	10 DEG	10 DEG

for Flights 1 and 2. This information is used to nondimensionalize stability and control derivatives.

Side-force surfaces capable of producing 1/2 q lateral acceleration for full deflection at 105 KIAS were added in recent years. In conjunction with this modification, the rudder area was increased. An important goal of this research was to identify the side-force surface control derivatives. Moments of inertia were modified to reflect the weight and position of these surfaces.

No actual measurements were made to determine the aircraft gross weight and moments of inertia. Such an experiment would be of great benefit in light of the structural modifications made to the aircraft. In addition, no estimate of the cross moment of inertia about the longitudinal and lateral axes, I_{xz}, is available from previous research. I_{xz} appears in several elements of the fundamental matrix, A, and although an I_{xz} of zero

3 -19

simplifies the equations, this assumption may be too
restrictive and add to the variance in estimating these
derivatives.

Although theoretically, the minimization algorithm
should converge on a set of parameter estimates given zero
values of the initial estimates, convergence on the true
values of the parameters is dependent on initializing the
estimation program with a reasonably good set of à priori
parameter values (Ref 3,7,8).

Unpublished stability and control derivatives which
were estimated using analog matching techniques are
available for the VRA in its current configuration.
Reference 1, 2, and 19 (quoted in Ref 3) also provide
estimates for the Navion aircraft in various configurations.
The analog matching results proved to be adequate as
starting estimates.

The measurement error weighting matrix was established
for each set of control input time histories using the
method described in Chapter 2.

3.7 <u>Conclusions</u>

Data acquisition is a crucial aspect in a parameter

estimation process. The quality of the flight data directly effects the quality of the parameter estimates. Dynamic errors in the sideslip angle and velocity measurement instruments suggest that these instruments should be repositioned. Low signal-to-noise ratios for accelerometers suggest that some form of filtering prior to transmission of these measurements is desirable. In calibrating instruments and control surfaces, specially constructed protractors and care in avoiding the linear limits of the telemetry and ground station will reduce scale factor and bias errors. Use of existing equipment on board the VRA can improve the quality of control inputs for use in parameter estimation. The discrete analog sampled data transmitted to the ground should be digitized directly to avoid the addition of noise and biases from processing data through several steps. Time delays introduced by the telemetry system can be corrected by interpolation as part of the data processing.

Time histories selected for use in estimating derivatives should have good signal-to-noise ratios and be free of equipment related anomalies. Accurate measurements of aircraft mass and inertia properties should be made prior to (or as part of) further research in parameter estimation. Published estimates and previous analog matching results

3 -21

make good initial estimates for the estimation program.

Chapters 4 and 5 discuss the lateral-directional and longitudinal stability and control derivatives estimated using the Modified Maximum Likelihood Estimation program.

3 -22

4. LATERAL-DIRECTIONAL DERIVATIVE DETERMINATION

The VRA lateral-directional derivatives were estimated using twenty time histories representing four basic control inputs: aileron pulses, rudder doublets, side-force surface pulses, and side-force surface doublets. The measured quantities were sideslip angle, roll rate, yaw rate, bank angle, lateral acceleration, aileron deflection, rudder deflection, and side-force surface deflection. The results of parameter estimation runs using these time histories were used to generate statistics describing the quality of the estimates. Initially, the variances of all estimates were high, so a number of procedures were use to determine the quality of the data and to reduce the variance. Results were separated by type of input and initial direction of the primary control surface. Because the variances in certain derivatives were reduced by separating runs, the effects of poor signal-to-noise ratios and nonlinear aircraft responses were documented.

Four initial runs indicated deficiencies in the data. Next, aileron input time histories were used to generate a set of starting values for the rudder time history estimates and to estimate aileron control derivatives. Rudder input

time histories were used holding aileron control derivatives fixed since the signal-to-noise ratio of aileron deflections in these time histories was small. Using the aileron and rudder control derivatives already estimated from previous runs, estimates were made using the side force surface input time histories. Here both aileron and rudder control derivatives were held fixed. From these runs, an overall set of estimates emerged, and the set was compared with results from other studies.

4.1 Initial Runs

Lateral-directional parameter estimation began with data from Flight 1. Control inputs used included aileron pulses, rudder doublets, and side-force doublets. Deflection of the side-force surfaces produced rudder and aileron deflections as well, due to a side-force-surface-to-rudder interconnect, and a side-force-surface-to-aileron interconnect. Parameter estimation using each type of input pointed to certain deficiencies in the data. Using a 5-sec time history of a 4-deg aileron pulse, the minimization algorithm diverged. The minimization for a 6-sec time history of a ±2.5-deg rudder doublet also diverged. The

4 - 2

signal-to-noise   ratios   for   these   control   inputs   were
approximately 8 and 5 for a noise band of 1/2 deg for   both.
Larger   amplitude   inputs   resulted   in   the   minimization
algorithm converging upon a set of estimates.   The estimates
from four time histories, two aileron pulses (+   7-deg   and
-10.7-deg, respectively), a side-force surface pulse of
-8.5-deg, and a series of side-force surface doublets
(±2.5-deg each), are presented in Table 4 along with the
standard deviation as a percentage of the estimate.

TABLE 4.LATERAL DIRECTIONAL DERIVATIVE ESTIMATES AND PERCENT
STANDARD DEVIATIONS FOR SEPARATE CONTROL SURFACE INPUTS

	Initial Runs	Aileron Pulses	Rudder Doublets	Side Force Surface Flt.1	Flt.2
C_{Y_β}	-.7878	-.7795	-.8758	-1.002	-1.155
	38.3	25.1	10.7	33.9	30.9
$C_{Y_{\delta a}}$	-.0812	.0230	------	------	.1667
	206.8	96.9			267.2
$C_{Y_{\delta r}}$	.2043	-.0790	.3634	------	.2306
	260.7	293.5	8.6		127.7
$C_{Y_{\delta sf}}$	.0861	-.3252	-.1888	.4499	.5837
	305.8	49.0	229.3	16.0	14.7

4 - 3

TABLE 4. (CONTINUED).

	Initial Runs	Aileron Pulses	Rudder Doublets	Side Force Flt.1	Surface Flt.2
C_{l_β}	-.0823	-.0892	-.1106	-.1232	.0877
	19.0	16.0	19.7	14.5	42.2
C_{l_p}	-.5012	-.5609	-.6376	-.6858	-.5562
	20.8	8.8	22.3	21.4	33.0
C_{l_r}	.0700	.1103	.1088	.0201	.1424
	199.6	61.3	15.8	468.0	96.2
$C_{l_{\delta a}}$	-.0709	-.1818	------	------	-.1272
	87.7	13.1			17.6
$C_{l_{\delta r}}$	-.0472	-.0379	.0246	------	.0246
	43.1	60.5	5.2		4.1
$C_{l_{\delta sf}}$	.0117	.0457	.1152	.0069	.0040
	270.5	93.9	36.2	121.2	441.2
C_{n_β}	.0875	.0745	.0751	.0751	.0900
	24.6	18.4	20.7	15.3	25.0
C_{n_p}	.1051	.0865	-.0935	-.1327	-.1755
	268.4	23.0	53.0	9.2	76.2
C_{n_r}	-.1310	-.1211	-.1556	-.2168	-.0951
	14.5	21.0	14.6	51.1	101.8
$C_{n_{\delta a}}$	-.0109	-.0196	------	------	-.0281
	62.3	30.1			60.6
$C_{n_{\delta r}}$	-.0019	-.0111	-.0974	------	-.0710
	2112	362.9	4.3		102.3
$C_{n_{\delta sf}}$	-.0020	.0150	-.0029	.0430	.0430
	768.	125.7	980.0	11.4	17.1

The scatter in the derivatives is excessive. Because of the variance in all derivatives, especially the angle-of-attack derivatives, the angle-of-attack derivatives were not estimated in subsequent runs. These derivatives are normally neglected when decoupling the modes of motion into a longitudinal set and a lateral-directional set. The side-force-surface-to-rudder interconnect prevented estimation of the side-force surface and rudder control derivatives independently. A second test flight was proposed using no interconnect between the surfaces. In the absence of new data, the rudder control derivatives were estimated from rudder alone input time histories and these derivatives were then fixed at estimated values. The side-force surface derivatives were then estimated from the Flight 1 side-force surface time histories.

The two aileron input time histories produced reasonably consistent stability derivative estimates. This suggested that separating estimates by sets according to the type of control would reduce the variance in some estimates. The information gained from each set was incorporated into the initial estimates for the next set. Table 5 lists the sequence of time histories used and the derivatives which were held fixed.

4 - 5

TABLE 5. SEQUENCE OF TIME HISTORIES USED IN ESTIMATING THE LATERAL-DIRECTIONAL DERIVATIVES.

CONTROL	NUMBER OF TIME HISTORIES	DERIVATIVES HELD FIXED
AILERON	7	-----
RUDDER	4	$C_{Y_{\delta a}}, C_{l_{\delta a}}, C_{n_{\delta a}}$
FLT.1 SIDE FORCE SURFACE	3	$C_{Y_{\delta a}}, C_{Y_{\delta r}}, C_{l_{\delta a}}, C_{l_{\delta r}}, C_{n_{\delta a}}, C_{n_{\delta r}}$
FLT.2 SIDE FORCE SURFACE	6	-----

The side-force coefficients, C_{Y_p} and C_{Y_r} were not calculated because the contribution of angle-of-attack to the dimensional quantities, Y_p and Y_r, could not be accurately removed.

4 - 6

4.2 Estimates Using Aileron Input Time Histories

Seven aileron pulse time histories with deflections of 7-deg or more were used to estimate the VRA stability and control derivatives. Table 4 summarizes the average estimates and associated standard deviations expressed as precentages of the mean values. The variances of all stability derivatives except C_{n_r} were reduced. Only C_{l_p} had a standard deviation less than 10 percent however.

The Dutch roll mode was not excited sufficiently to produce perturbations in yaw rate and sideslip angle time histories that had high signal-to-noise ratios. Maximum sideslip perturbations were less than 3.5 deg and maximum yaw rate perturbations were less than 6.6 deg/sec. In addition, a dynamic instrument error in the sideslip vane, discussed in Chapter 3, makes side-force derivative estimates questionable. Although the estimated lower bounds of the standard deviations (Cramer-Rao bounds) of these traditional Dutch roll parameters are lower than the standard deviations obtained, it must be remembered that the actual time histories and the analytical model are subject to measurement errors, turbulence inputs, and modeling errors. The presence of modeling errors is recognized

immediately when the estimates are grouped by direction of aileron pulse. The variances in C_{Y_β}, C_{l_p}, C_{l_r} and $C_{l_{\beta a}}$ are reduced when estimates are separated into groups by direction of aileron pulse. These estimates are separated by more than two standard deviations (Appendix A). A 5-percent aileron scale factor correction that represents a more linear response of the ailerons did not significantly reduce the separation of the estimates. More research is needed to investgate this seemingly nonlinear response to aileron inputs. A nonlinear model would be needed to identify an asymmetric aircraft response.

Figures 6 and 7 illustrate some of the difficulties in using aileron time histories. Time history matches of roll rate and bank angle generally are good. Sideslip angle matches are poor, reflecting the dynamic error in the measurements and the low signal-to-noise ratio, and possibly a poor match for the Dutch roll damping derivative, C_{n_r}. The lateral acceleration matches are fair, usually following gross trends well, but the noise in the control measurements, especially for the side-force position, is noticeable in these time histories. A heading angle measurement might be used in place of the sideslip measurement.

FIGURE 6. COMPARISON OF FLIGHT 1 DATA(M) WITH TIME HISTORIES(E) COMPUTED USING THE PRESENT STUDY STABILITY AND CONTROL DERIVATIVES FOR A POSITIVE AILFRON PULSE INPUT. (ABSCISSA IS TIME IN SEC)

4 - 9
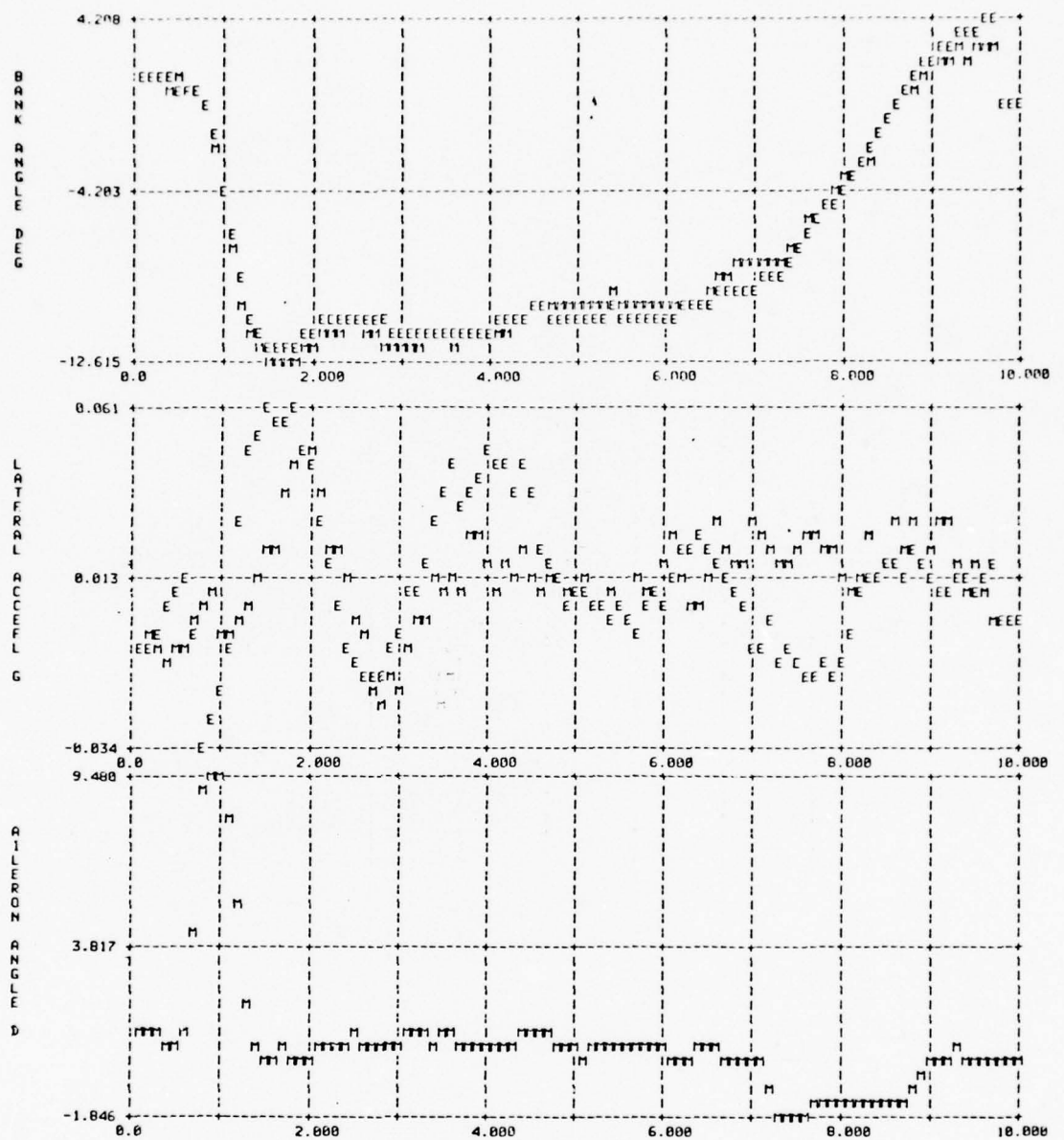
FIGURE 6. (CONTINUED).

4 -10
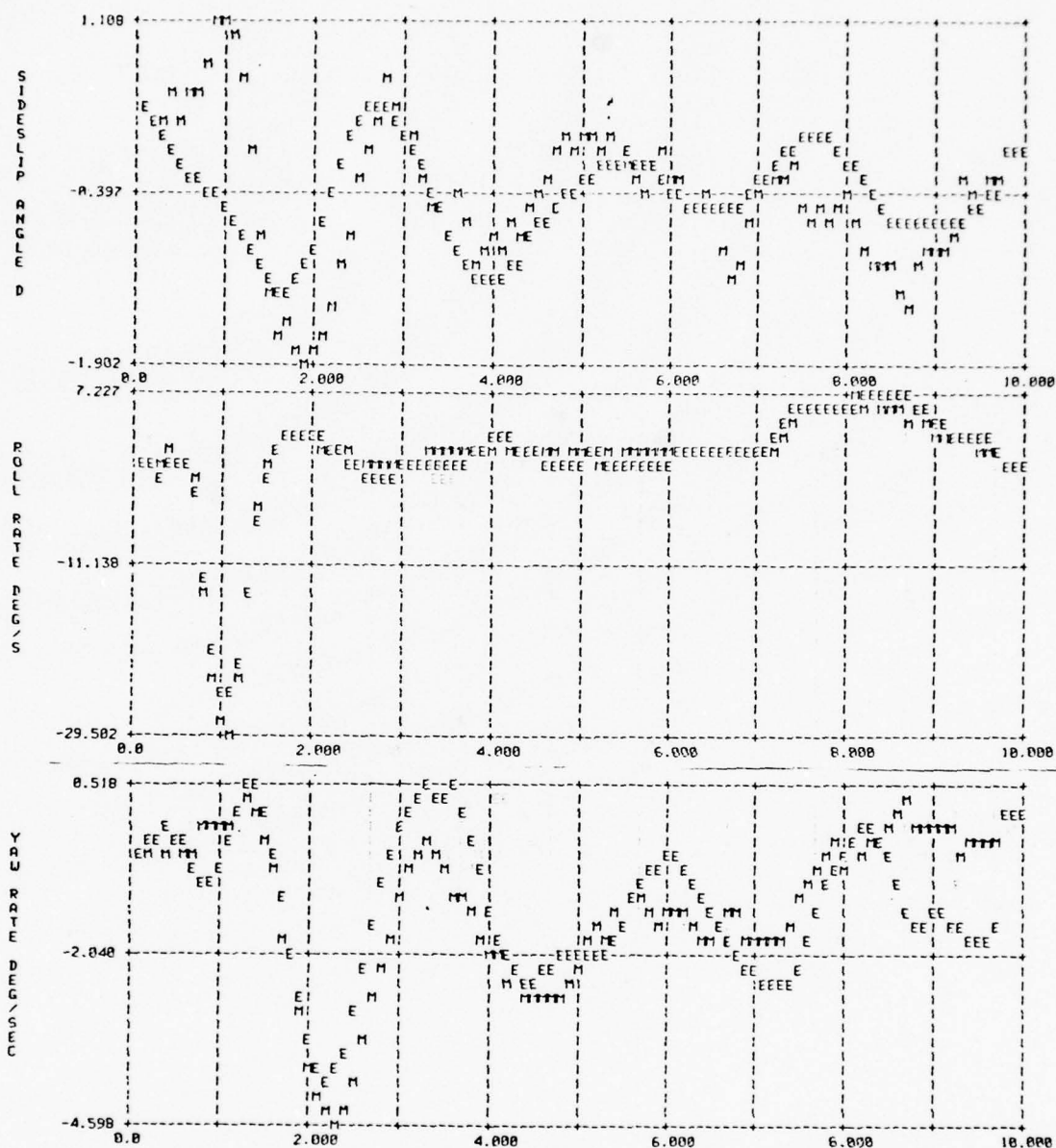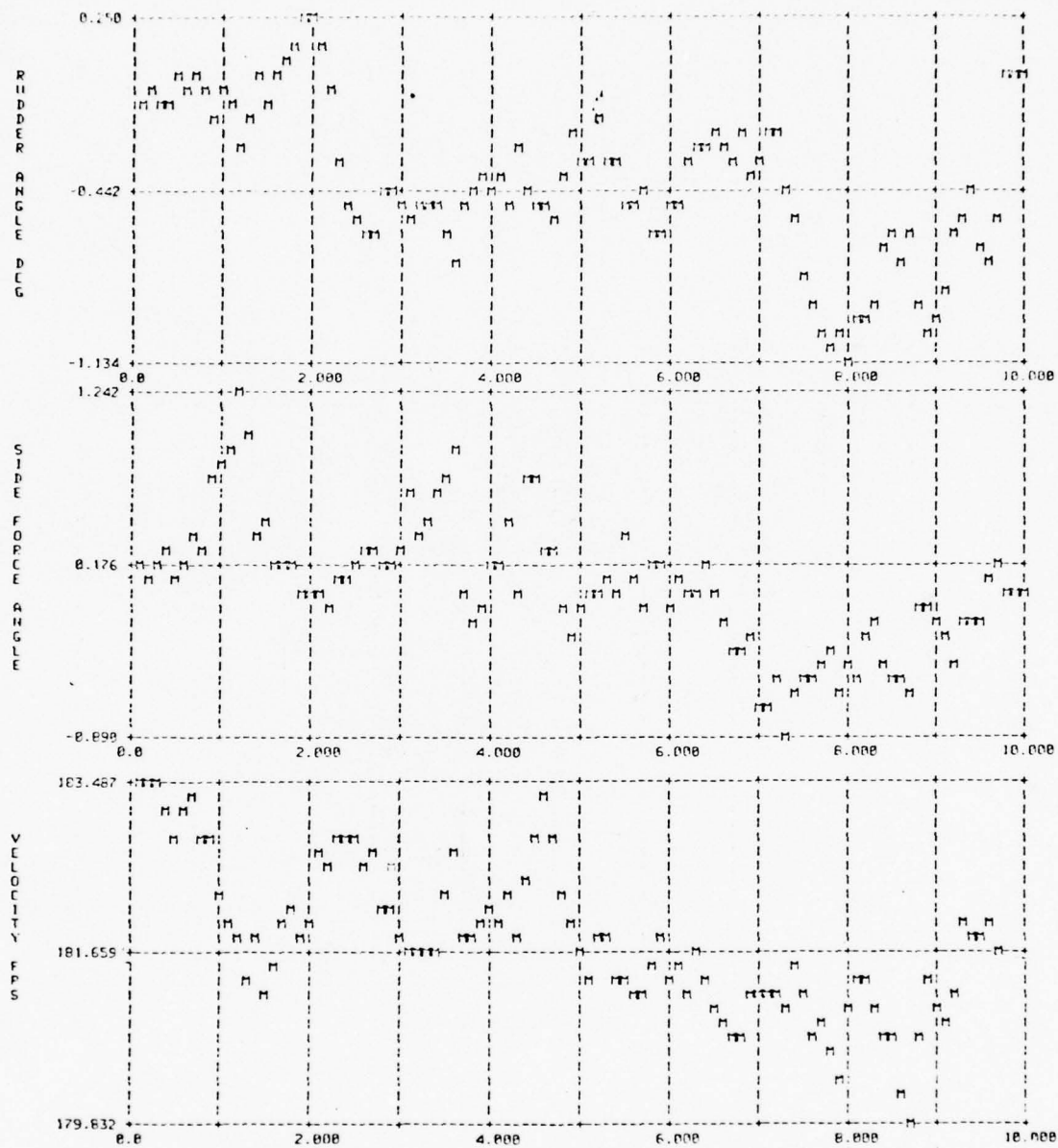
FIGURE 6. (CONCLUDED).

4 - 11
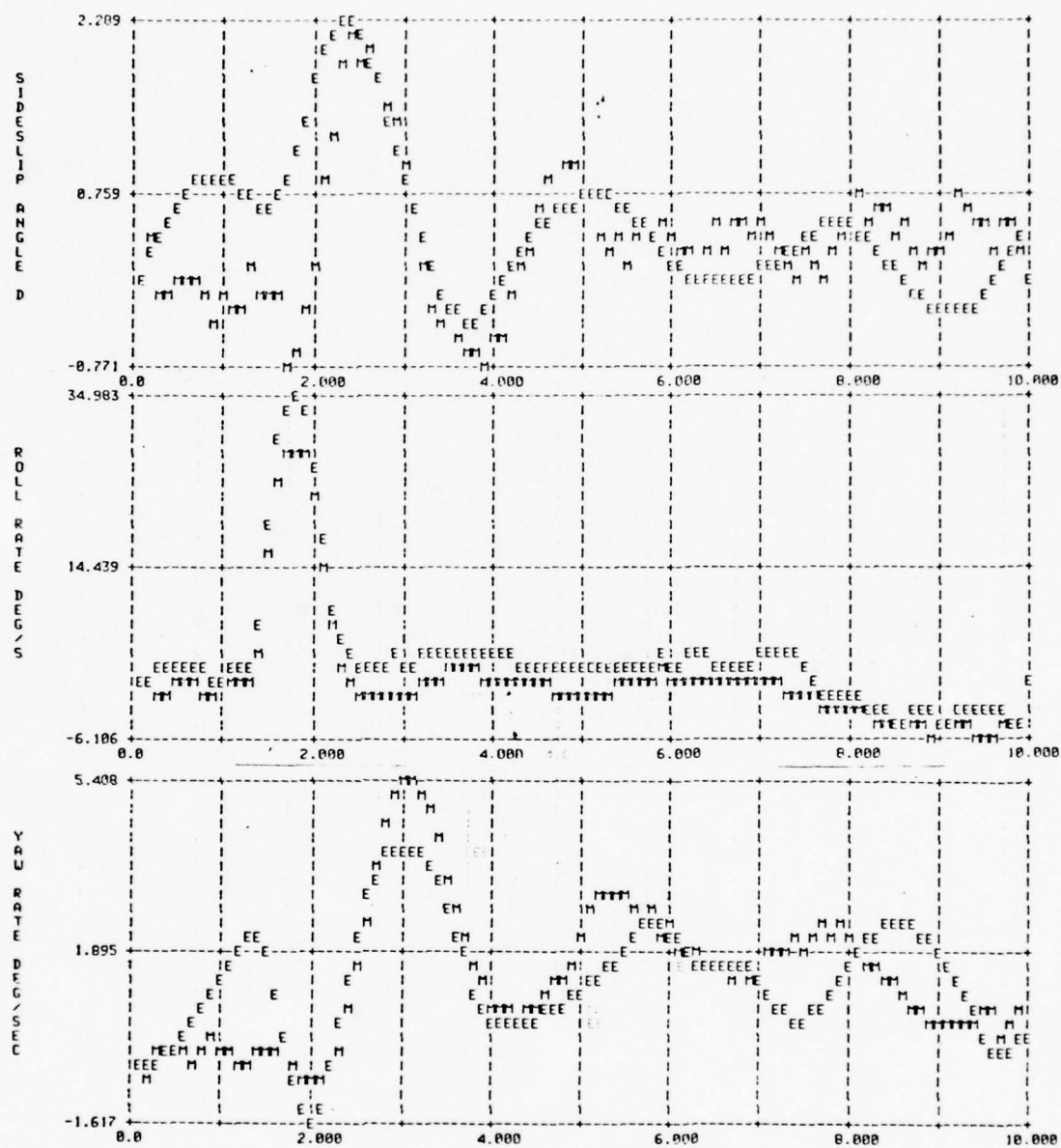
FIGURE 7.   COMPARISON   OF   FLIGHT   1   DATA(M)   WITH   TIME
HISTORIES(E)   COMPUTED USING THE PRESENT STUDY STABILITY AND
CONTROL DERIVATIVES FOR   A   NEGATIVE   AILERON   PULSE   INPUT.
(ABSCISSA IS TIME IN SEC)

4 -12
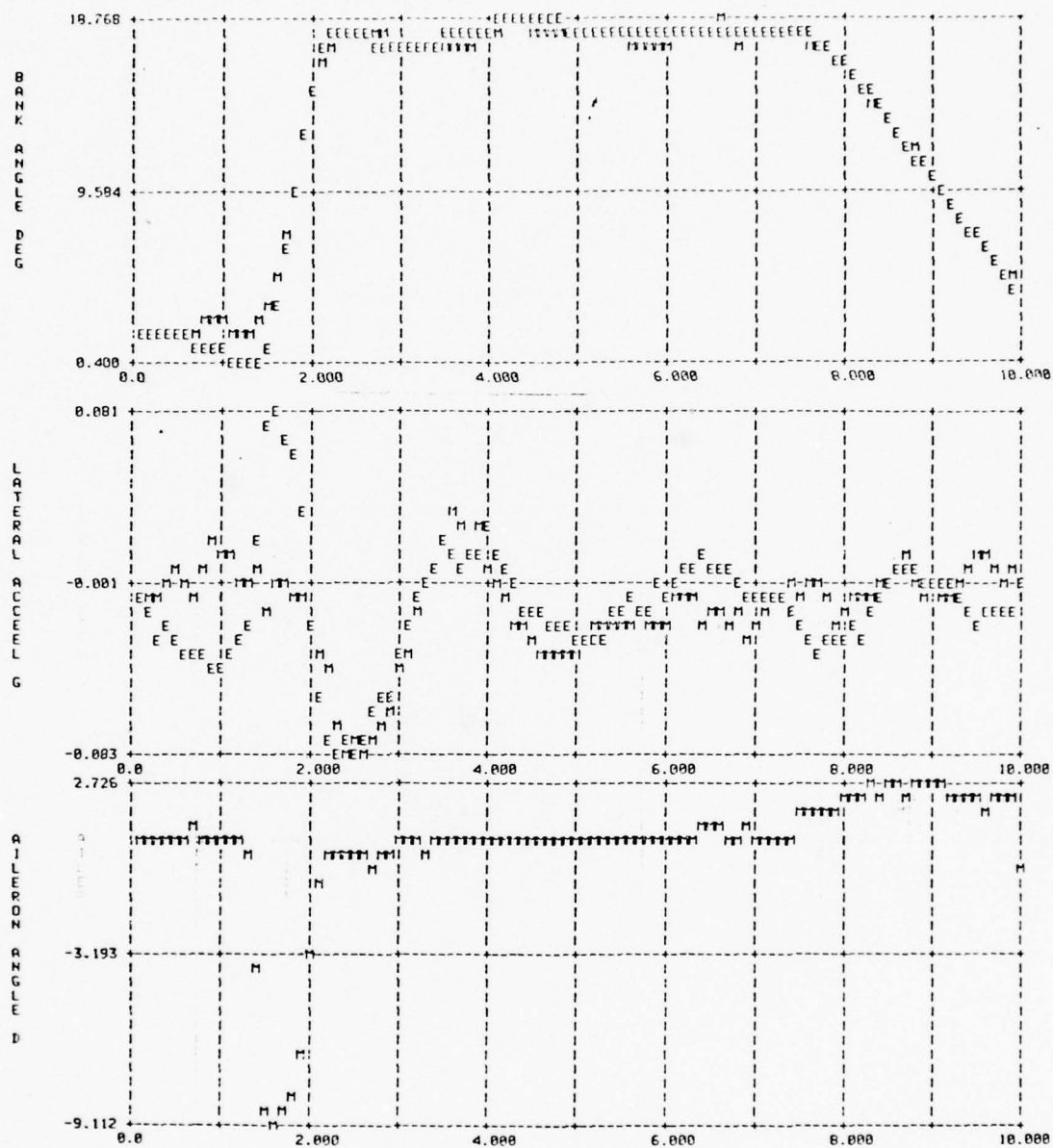
FIGURE 7. (CONTINUED).
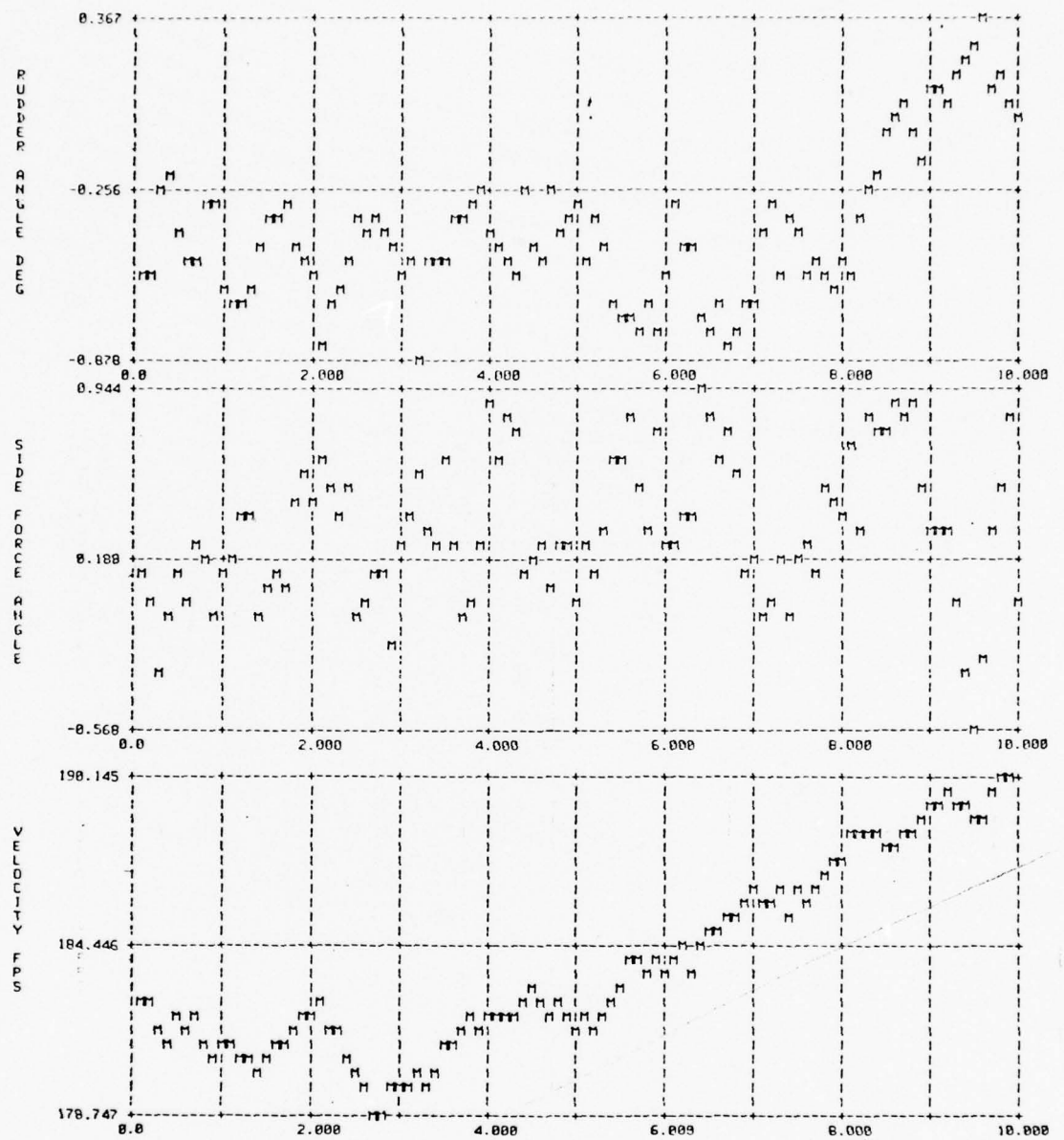
FIGURE 7. (CONCLUDED).

4 -14

It was expected that rudder inputs would better excite the Dutch roll mode and thus reduce the variance in several stability derivatives.

4.3 Estimates Using Rudder Input Time Histories

Four rudder doublet ($\pm$2.8-deg to $\pm$6.3-deg) input time histories produced stability and control derivatives with reduced variances in most cases. Table 4 summarizes the estimates using these time histories. The major reductions in variances were in derivatives whose associated state perturbations were much larger than those associated with the aileron input time histories (C_{Y_β}, C_{l_r}, C_{n_r}).

In order to determine the best use of the estimates obtained from the aileron input time histories, three runs were made evaluating the benefit of weighting changes in estimates from à priori values. The first run used as starting values the estimates obtained from the aileron input time histories. The second run also used these starting values and, in addition, weighted excursions from these values using the following equation to calculate the weighting term for the D2 matrix (Eq 26):

4 -15

$$d_{ij} = \frac{n-1}{D^2 \sigma_{ij}^{(1)}}$$

(40)

where σ_{ij}^2 is the variance in the ith row/jth column derivative of the A or B matrix, and n is the number of aileron input time histories used in estimating that derivative. A third run used the same starting values and a priori weighting, holding the aileron control derivatives fixed at the previous estimates (i.e., the average of the estimates for both directions). Since these estimates were obtained using aileron inputs with much superior signal-to-noise ratios by comparison to the deflections obtained during the rudder input time histories, these estimates were the best obtainable set. This conclusion was confirmed by the large departure of the aileron control derivatives from their previously estimated values for the first two runs, and also the four- to five-fold increase in the estimated lower bounds of the standard deviations of these derivatives (Cramèr-Rao bounds).

Side-force derivatives for Runs 2 and 3 changed less than ten percent from estimates obtained from Run 1.

4 -16

Rolling moment derivatives changed from 30 to 50 percent for Run 2 and from 50 to 250 percent for Run 3. All changes were towards the previous estimates, and the largest changes were for $L_{\delta a}$ as expected. Cramer-Rao bounds increased somewhat for these derivatives, but it must be remembered that these bounds represent the lower bound of the standard deviations obtainable from the time history used. The previous estimates came from time histories with lower Cramer-Rao bounds than those for Run 1, so these estimates have higher confidence levels.

The yawing moment derivatives for Run 2 were within ten percent of those for Run 1. N_p For Run 3, decreased 70 percent towards its initial estimate. N_β increased 51 percent and N_r decreased 34 percent. $N_{\delta r}$ increased only 5 percent. For all four derivatives, however the Cramer-Rao bounds decreased from Run 1 to Run 3 (11 percent decrease for $N_{\delta r}$), indicating that the confidence in the derivatives increased by fixing the aileron control derivatives.

Estimates were separated into groups having the same initial rudder deflection. Reductions in variance and estimates separated by two standard deviations were obtained for C_{l_β}, C_{l_p}, $C_{l_{\delta r}}$, C_{n_β} and C_{n_p} (Appendix A). These results again indicate that the VBA roll response is

4 -17

nonlinear and that its yawing response may be as well. More rudder input data would aid in establishing a yawing nonlinearity. These results do reenforce the need for research on an improved analytical model.

There was little or no degradation in the time history matches from Run 1 to Run 3. All state time histories were matched very well, and the sideslip angle and lateral acceleration matches were far superior to the lower amplitude aileron input time history matches. The dynamic error in the sideslip angle measurement was not apparant for angle-of-attack perturbations of 4 degrees and pitch rate perturbations of 3.5 degrees/second.

Figure 8 shows matches for a rudder input time history using the final set of estimates from this study. Because sideslip angle, yaw rate, and lateral acceleration perturbations are much larger than those for aileron time histories (7-10-fold increase) these matches are much better than the previous matches. With the Dutch roll mode-related stability derivatives and rudder control derivatives better identified, the side-force surface input time histories were used for parameter estimation.
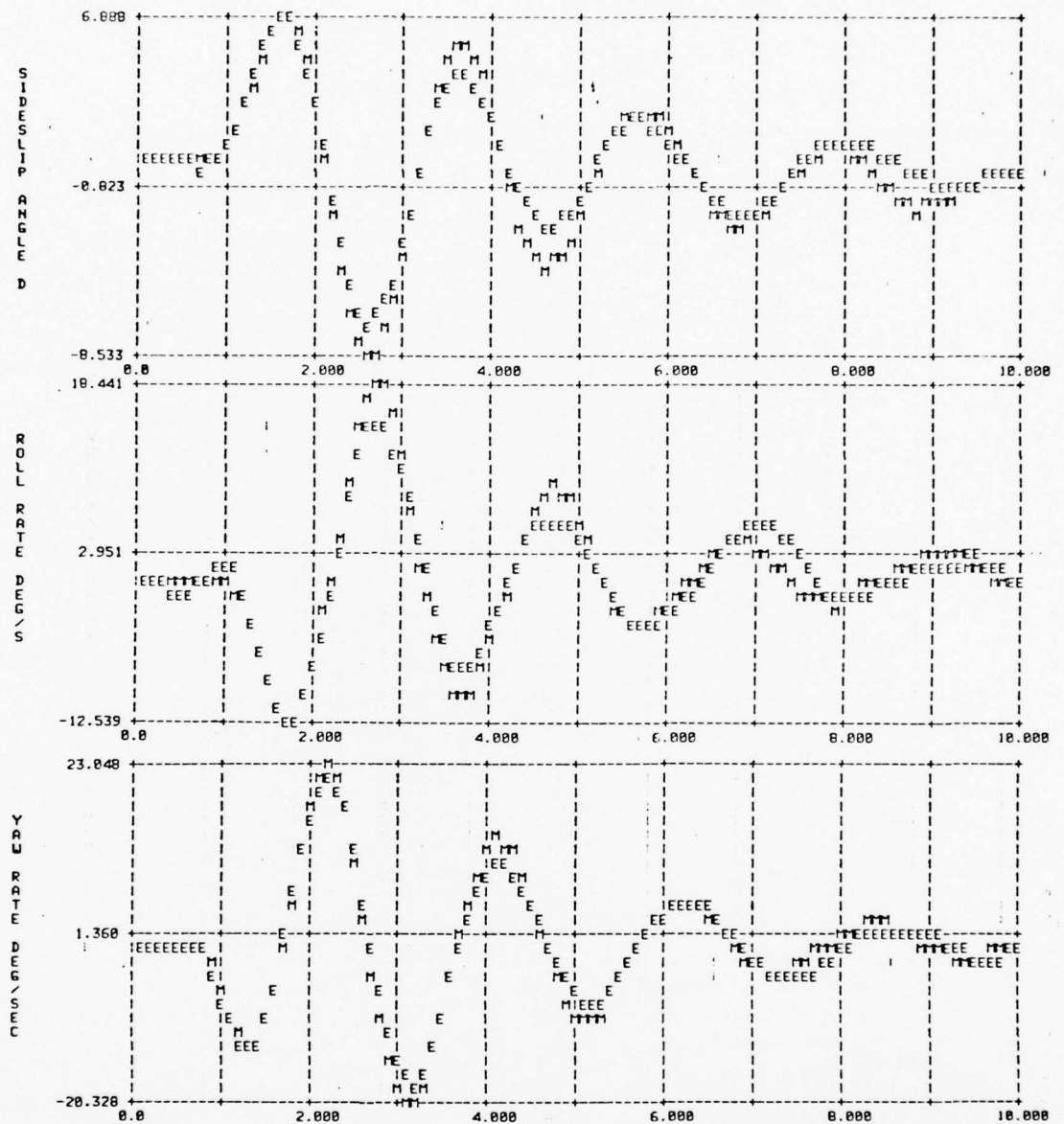
FIGURE 8. COMPARISON OF FLIGHT 1 DATA(M) WITH TIME HISTORIES(E) COMPUTED USING THE PRESENT STUDY STABILITY AND CONTROL DERIVATIVES FOR A RUDDER DOUBLET INPUT. (ABSCISSA IS TIME IN SEC)

4 -19
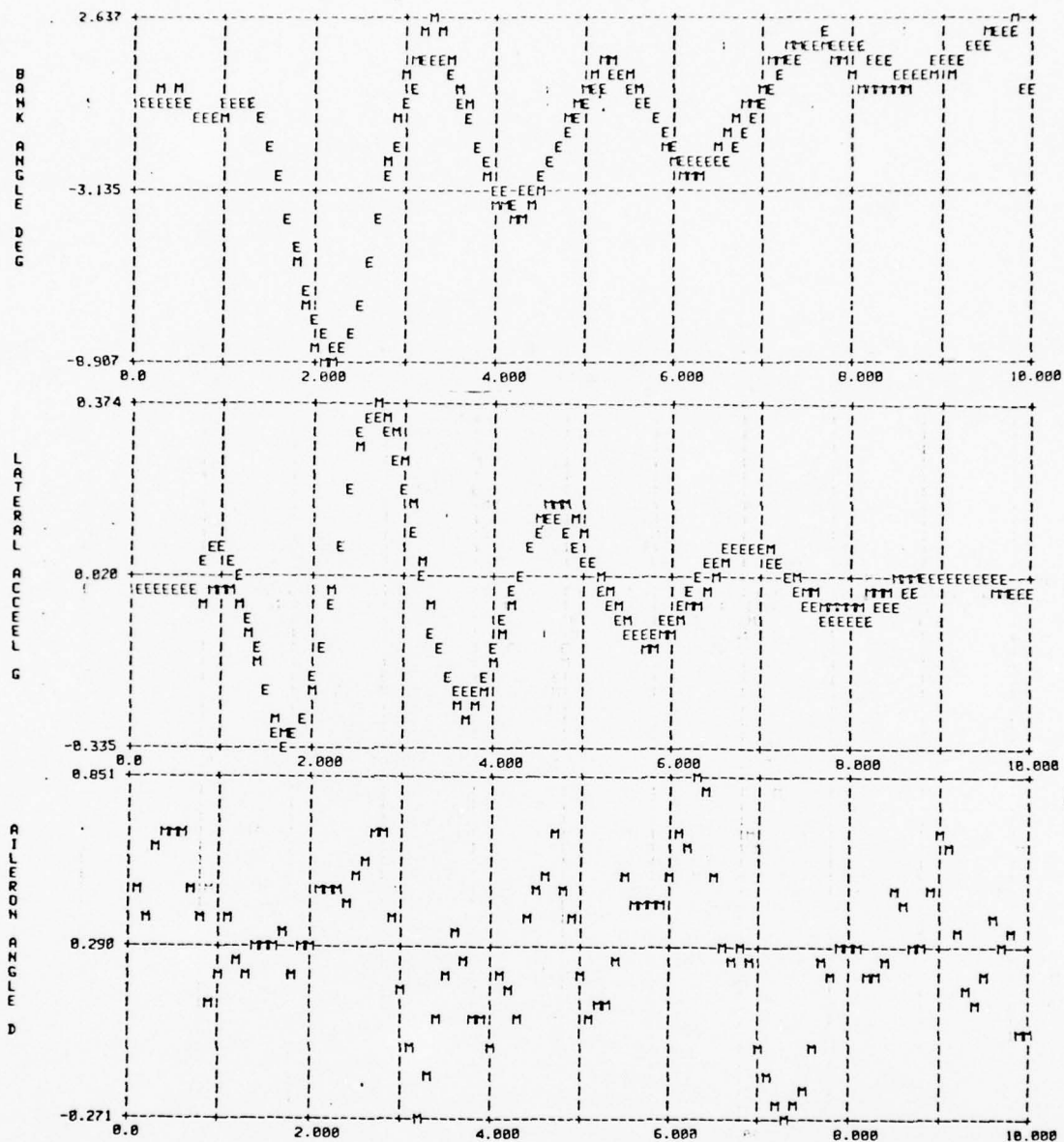
FIGURE 8. (CONTINUED).

4 -20
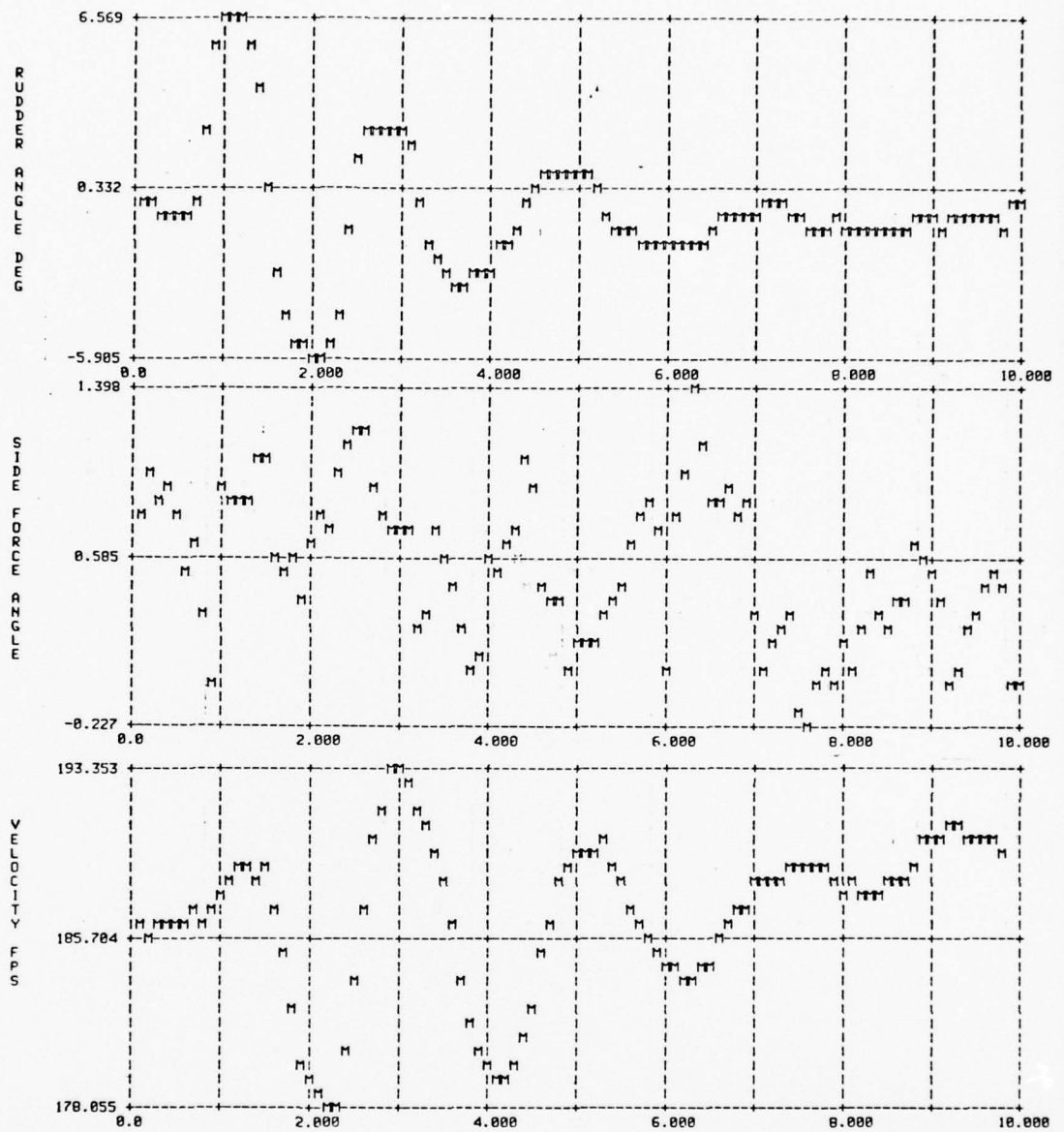
FIGURE 8. (CONCLUDED).

4 -21

4.4 Estimates Using Side-Force Surface Input Time Histories

Nine side-force surface input time histories were used to estimate the VRA'S stability and control derivatives. Three were previously used during the initial runs. These were from Flight 1, in which a side-force-surface-to-rudder interconnect was used. Six were from Flight 2, for which the interconnect was removed. No measurement of roll rate was available on Flight 2 due to an instrument failure, and the lateral acceleration measurement was poor. Consequently, the estimates were degraded. Table 4 summarizes the results of these estimates.

Aileron and rudder control derivatives were held fixed for the Flight 1 time histories. Starting values for the derivatives to be estimated were based on estimates obtained from the aileron and rudder inputs time histories. A priori weighting was used again, with the weighting matrix elements being calculated in the same manner as for estimates using rudder input time histories.

The à priori weighting for Flight 2 data was based on the Flight 1 side-force surface input results for side-force derivatives as well as previous estimates. All control derivatives were estimated.

For these two sets of time histories the C_{Y_β} estimate is poor (Table 4) due to low signal-to-noise ratios for sideslip angle and lateral acceleration. The largest sideslip angle perturbation for any of the nine time histories was 7.5-deg. This compares with the maximums of from 10 to 15 deg which were obtained with rudder doublet inputs. Greater care in input design must be taken to accrue the maximum benefit from the side-force surfaces in identifying side-force stability derivatives.

The side-force-surface-to-aileron interconnect used on Flight 1 effectively cancelled side-force surface rolling moments, since Flight 1 time histories did not excite the roll mode to sufficient amplitudes. Cramer-Rao bounds for rolling moment stability derivatives usually were greater than 14 percent of the estimates, with L_r bounds greater than 75 percent. This indicates a low confidence level for these estimates. No roll rate measurements were available from Flight 2 time histories. Cramer-Rao bounds all were greater than 10 percent of the estimates of L_β, L_p and L_r. These derivatives, therefore, were not determined from the side-force surface input time histories available.

Yawing moment stability derivative estimates were not as accurate as was expected. C_{n_β} was identified reasonably

4 -23

well, with standard deviations near the Cramèr-Rao lower bounds. The standard deviation for C_{n_p} from Flight 1 time histories is surprisingly small, in fact, it is smaller that the estimated Cramèr-Rao bound. The lack of roll rate measurements and the poor lateral acceleration measurements for Flight 2 contribute to the variance in C_{n_p} and C_{n_r}.

The side-force surface control derivative estimates from Flight 2 reflect the estimates from Flight 1 through the D2 weighting matrix (Eq 28). In addition, they are not perfectly correlated with aileron and rudder derivatives. The $C_{Y_{\delta sf}}$ estimate is therefore accepted over the estimate from Flight 1 time histories. The very large variance in $C_{l_{\delta sf}}$ the corresponding large variance predicted by Cramèr-Rao bounds, and the near zero estimate indicate that this derivative was not determinable from the data available. Again, the side-force-surface-to-aileron interconnect used during Flight 1 and the failure to measure roll rate during Flight 2 contribute to the large variance.

Figures 9 and 10 are Flight 2 time history matches using present study derivatives. In Figure 9, a 6-sec side-force surface pulse produces large state perturbations and the matches are reasonably good. The sideslip angle measurement in Figure 10 suggests that the measurement error
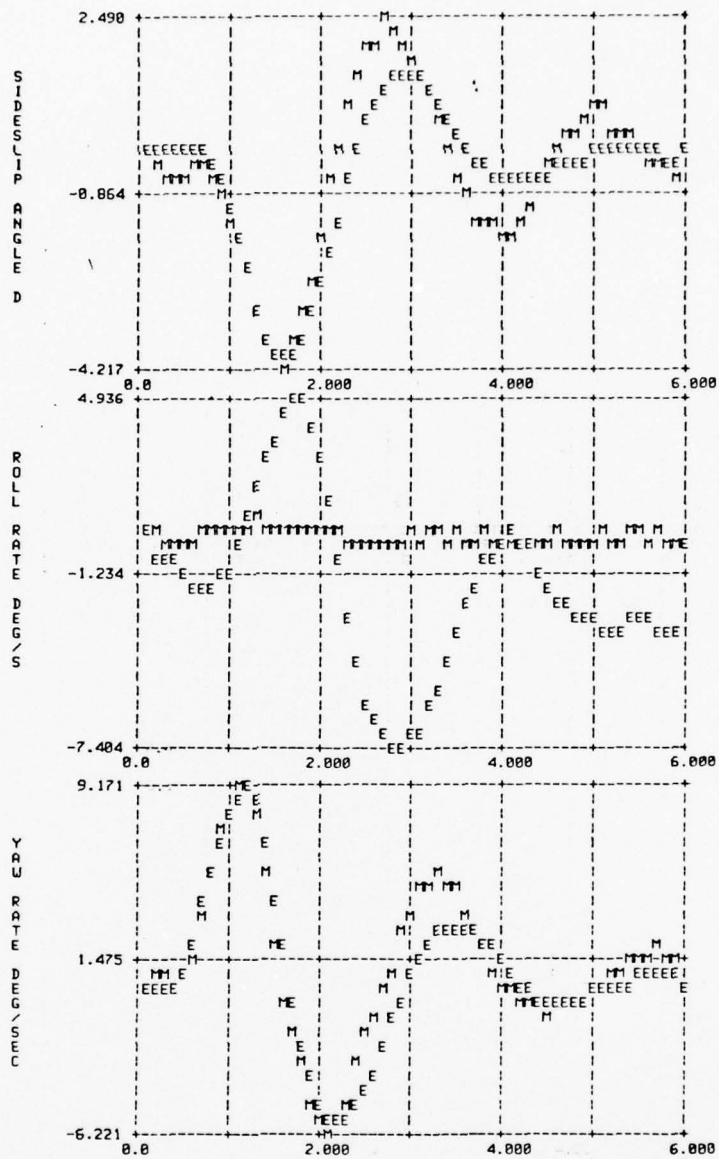
FIGURE 9. COMPARISON OF FLIGHT 2 DATA(M) WITH TIME HISTORIES(E) COMPUTED USING THE PRESENT STUDY STABILITY AND CONTROL DERIVATIVES FOR A SIDE FORCE SURFACE PULSE INPUT. (ABSCISSA IS TIME IN SEC)

4 -25
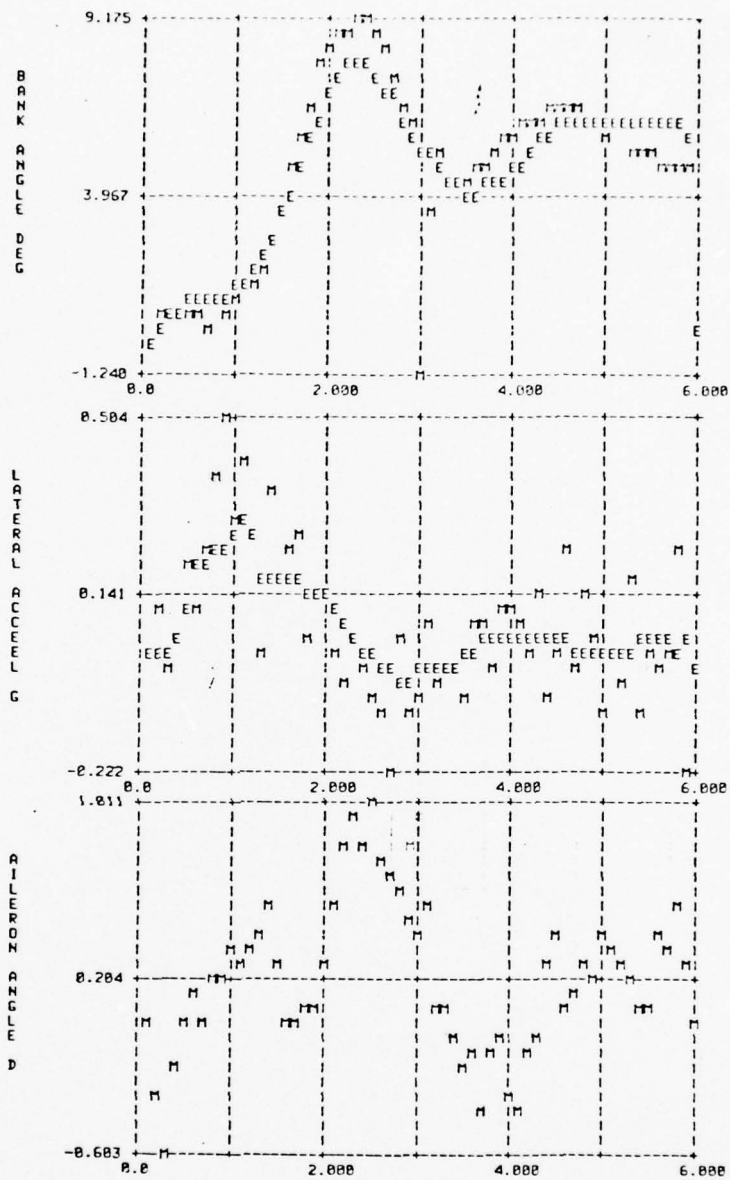
FIGURE 9. (CONTINUED).

4 -26
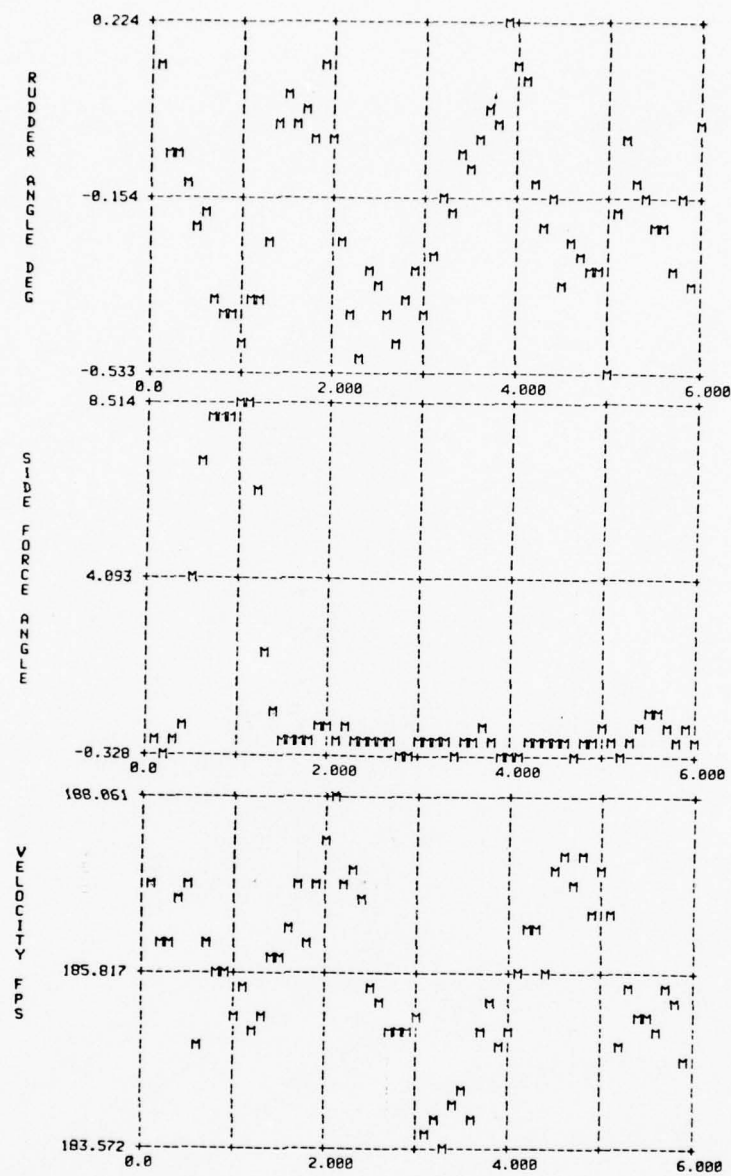
FIGURE 9. (CONCLUDED).

4 -27
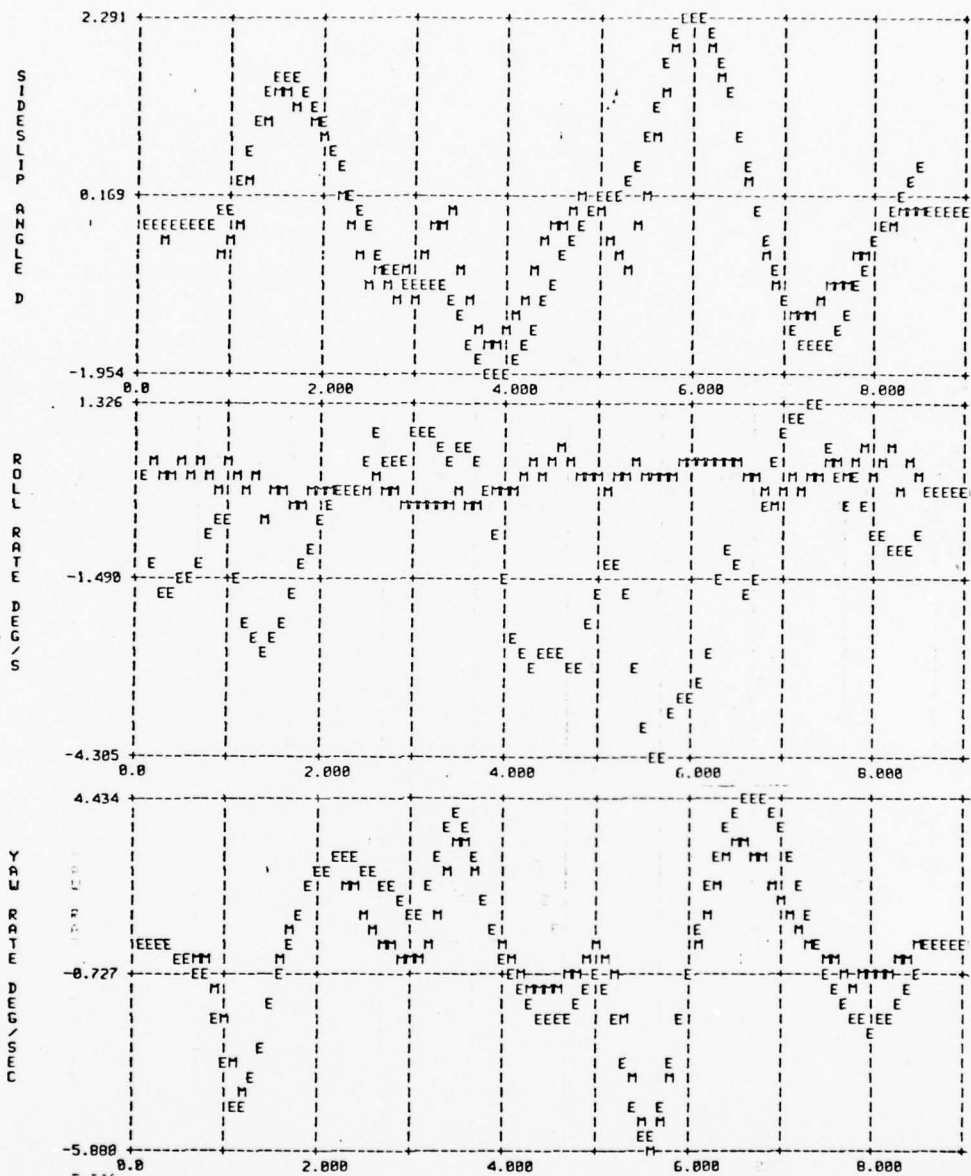
FIGURE 10. COMPARISON OF FLIGHT 2 DATA(M) WITH TIME HISTORIES(E) COMPUTED USING THE PRESENT STUDY STABILITY AND CONTROL DERIVATIVES FOR A SIDE FORCE SURFACE DOUBLET INPUT. (ABSCISSA IS TIME IN SEC)
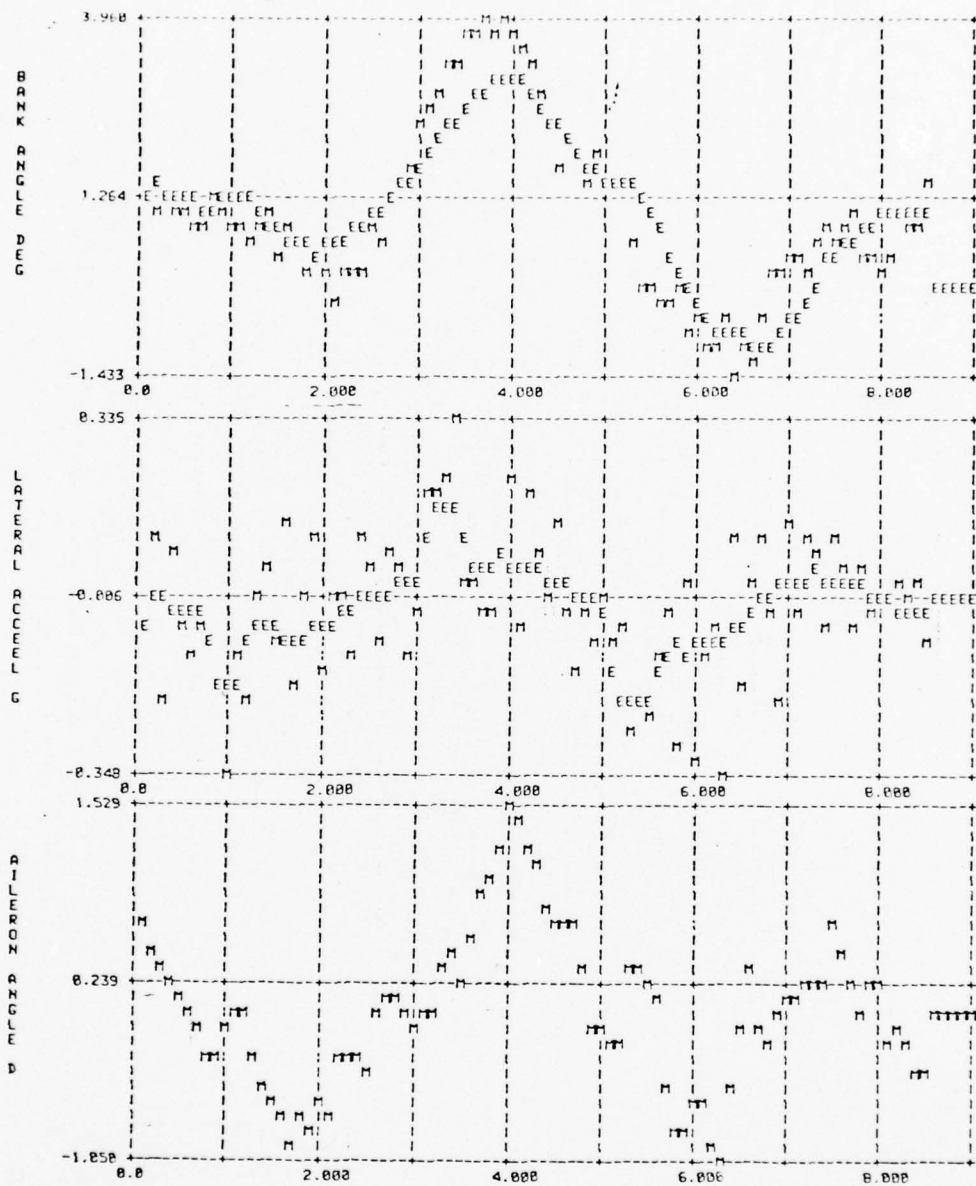
4 -28

FIGURE 10. (CONTINUED).
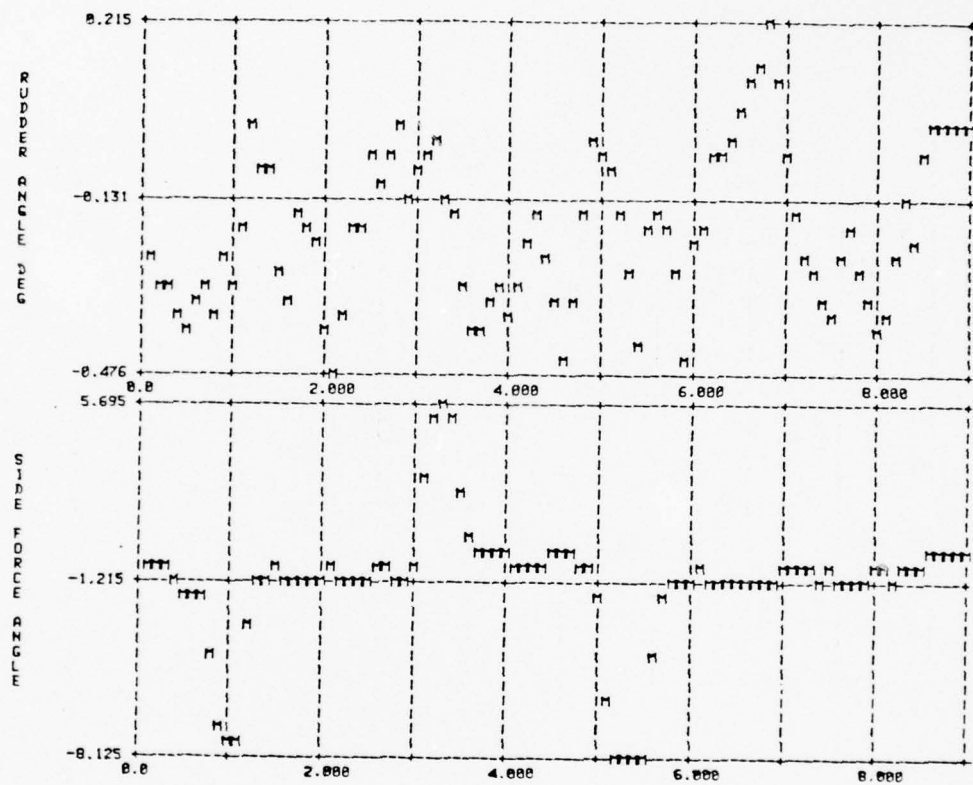
4 - 29

FIGURE 10. (CONCLUDED).

4 -30
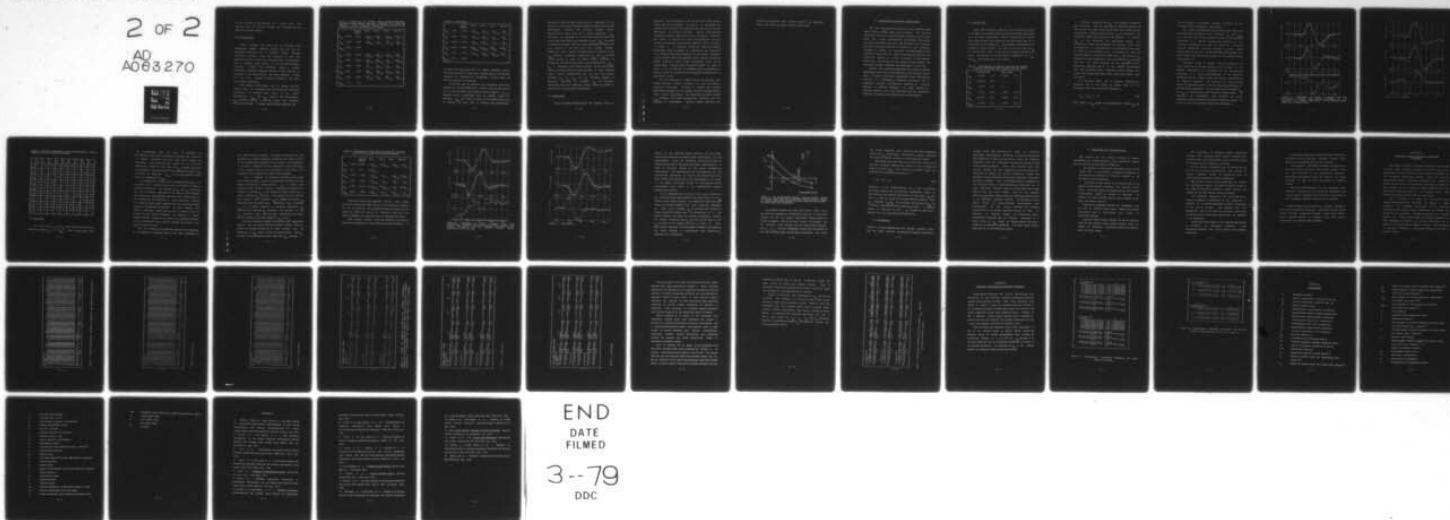
is not corrected by the addition of a second vane. The dynamic error is clearly visible and in phase with the side-force surface pulses.

4.5 Final Results

Table 6 compares the final set of estimates with unpublished analog matching results for the VRA and published estimates for a standard Navion (without side-force panels). They are presented to give some indication of the variance in estimates among investigators and to identify some effects of the VRA modifications. Reference 3 results were estimated using a maximum likelihood estimation approach similar to this study on the VRA prior to the modification. The analog matching results are the most current estimates available and offer interesting comparisons.

Rudder control derivatives for the analog matching results were not estimated, but they represent analytical corrections to estimates made prior to the rudder modification. $C_{l_{\delta r}}$ and $C_{n_{\delta r}}$ compare very well, however. $C_{Y_{\delta r}}$ estimates from Ref 3 are much higher than estimates from other sources. A similar relationship holds for the

4 -31

TABLE 6. COMPARISON OF PRESENT STUDY LATERAL DIRECTIONAL DERIVATIVES WITH ANALOG MATCHING ESTIMATES AND PUBLISHED RESULTS. (SLASH INDICATES NAVION ESTIMATES PRIOR TO VRA MODIFICATIONS; 0 DEG FLAPS/20 DEG FLAPS)

		Analog Match	Ref.3	Ref.2	Ref.1	Ref.18
C_{Y_β}	-.8756	-.9176	-.60/-.74	-.61/----	-.80/-.77	-.56/----
$C_{Y_{\delta r}}$	.3634	.2145	.33/.68	----/----	.14/.14	.16/----
$C_{Y_{\delta sf}}$	.5837	.8717				
C_{l_β}	-.0980	-.0863	-.07/-.05	-.07/-.05	-.11/-.10	-.07/----
C_{l_p}	-.5660	-.5198	-.49/-.53	-.46/-.48	----/----	-.41/----
C_{l_r}	.1088	.0928	.11/.11	.07/.27	----/----	.11/----
$C_{l_{\delta a}}$	-.1851	.1576	.15/.16	.15/.15	.15/.09	.13/----
$C_{l_{\delta r}}$	.0246	.0254	.03/.01	----/----	.03/.02	.01/----
$C_{l_{\delta sf}}$	0.0	0.0				

4 -32

TABLE 6. (CONTINUED).

		Analog Match	Ref.3	Ref.2	Ref.1	Ref.18
C_{n_β}	.0837	.1033	.07/.08	.09/.08	.11/.13	.07/----
C_{n_p}	-.0865	-.0485	-.04/-.15	-.04/-.14	----/----	-.06/----
C_{n_r}	-.1556	-.1113	-.09/-.12	-.09/-.16	----/----	-.13/----
$C_{n_{\delta a}}$	-.0196	-.0039	∓004/∓002	∓005/∓001	∓005/0.0	∓004/----
$C_{n_{\delta r}}$	-.0974	-.1068	-.06/-.08	-.08/-.09	-.08/-.08	-.07/----
$C_{n_{\delta sf}}$	.0430	.0368				

estimate from this study and the analog matching result. The large variance in side-force surface control derivatives reflects the difficulties encountered in this study, and further research is indicated.

This study used the opposite sign convention from other studies for aileron deflection. Aileron control derivatives are in poor agreement with analog matching results. $C_{l_{\delta a}}$ is somewhat larger in magnitude than the analog result (17 percent). $C_{n_{\delta a}}$ is 5 times as large as the analog result and is opposite in sign (due to opposite sign convention).

4 -33

Additional runs were made using à priori weighting on the stability derivatives, holding rudder and side-force surface derivatives constant and allowing aileron control derivatives to vary with no à priori weighting. $C_{l_{\delta a}}$ decreased in magnitude to a value more consistent with the analog matching result and published values. $C_{n_{\delta a}}$ increased in magnitude, however, and this large favorable yaw effect was very visible in the yaw rate time history matches. Cramér-Rao lower bounds averaged around 10 percent of the $C_{n_{\delta a}}$ estimate. Reference 3 fixed both $C_{l_{\delta a}}$ and $C_{n_{\delta a}}$ at wind tunnel values in order to obtain better estimates of parameters correlated with these control derivatives (C_{l_p}, C_{n_p}). Additional runs holding aileron control derivatives fixed at analog matching values resulted in poor sideslip angle, lateral acceleration, and yaw rate time history matches. $C_{l_{\beta}}$, C_{l_r}, $C_{n_{\beta}}$, and C_{n_r} estimates doubled in magnitude (Appendix A) although C_{l_p} did decrease. Additional data using different aileron inputs are needed to improve the rolling moment derivatives.

4.6 <u>Conclusions</u>

Initial estimates demonstrated the dynamic error in

4 -34

sideslip angle measurements, and the need for large control inputs and state responses. The scatter in estimates was reduced when estimates were separated by type and by initial deflection of control surfaces. Control interconnects prevented accurate side-force surface derivative estimates for Flight 1, and lack of a roll rate measurement and poor lateral acceleration measurements degraded these estimates on Flight 2. An improved analytical model and reduced measurement noise is needed to investigate the nonlinear roll and yaw responses documented in this study. Reference 3 and 5 suggest model improvements, while optimal filtering and/or smoothing could reduce measurement noise in the current data. Heading angle information might be used in place of (or in addition to) sideslip angle measurements to prevent biases of the side-force derivative estimates due to instrument errors.

The poor agreement of aileron control derivatives with analog matching results indicates the need for further research in this area. Attempts to improve the aileron derivative estimates in the present research included fixing other control derivatives. This resulted in a still poorer $C_{n_{\delta a}}$ estimate. The large favorable yaw predicted was not verified by measurement. Sideslip angle, yaw rate, and

4 -35

lateral acceleration time history matches are generally
poorer than those for other control deflections.

5. LONGITUDINAL DERIVATIVE DETERMINATION

The VRA longitudinal derivatives were estimated using eight elevator doublet input time histories. The measured quantities used were angle-of-attack, velocity, pitch angle, pitch rate, normal acceleration, and elevator deflection. Parameter estimates from these time histories were averaged, and their variances indicate the quality of the estimates. Attempts to reduce the variances included fixing single derivatives from pairs of highly correlated derivatives and separating results by initial direction of the elevator deflection. The effects of poor signal-to-noise ratios and nonlinear aircraft responses were documented in this way.

Initial runs clearly demonstrated the dynamic velocity measurement error due to the location of the aircraft static ports. Attempts to estimate longitudinal force derivatives resulted in minimization algorithm divergence due to inadequate velocity perturbations produced by aircraft response to elevator doublets. For these reasons, the velocity equation in Eq 7 was neglected, and the associated stability and control derivatives were not estimated.

5 - 1

5.1 Initial Runs

Seven time histories (each of 5 sec duration) were used to estimate the stability and control derivatives associated with the short period mode. Table 7 summarizes the results from these initial runs along with standard deviations as a percentage of the estimates. Two immediate difficulties are evident in these results. The first is that the sign of C_{Z_q} is inconsistent with theory and its standard deviation is large. The second is that the relative magnitudes of $C_{Z_{\delta e}}$ and $C_{m_{\delta e}}$ are inconsistent with theory.

TABLE 7. LONGITUDINAL DERIVATIVE ESTIMATES AND PERCENT STANDARD DEVIATIONS FROM ELEVATOR DOUBLET INPUTS.

	Initial Runs		Final Runs	
C_{Z_α}	-3.6565	7.5	-5.6226	12.7
C_{Z_q}	18.9338	86.5	-----	
$C_{Z_{\delta e}}$	-1.1496	27.5	-----	
C_{m_α}	-.4068	24.9	-.6107	19.8
C_{m_q}	-18.5956	32.7	-7.8665	46.9
$C_{m_{\delta e}}$	-1.2776	25.5	-.8207	21.0

Reference 3 suggests that C_{z_q} is an important parameter for the Navion. Since the addition of side-force panels and the increase in rudder area should have little effect on the longitudinal stability derivatives, C_{z_q} was included in the analytical model and estimated to be positive. A positive C_{z_q} is not consistent with aerodynamic theory. The incremental normal force produced by positive pitch rate perturbations is primarily due to an increase in the angle of attack at the horizontal tail. An increase in angle of attack results in a negative normal force. The positive C_{z_q} estimate is also inconsistant with the negative C_{m_q} estimate (Ref 5). The large variance in the estimates of this derivative indicates that it is not readily determinable from the available data. Different control inputs, e.g., direct lift pulses from wing flaps, might help isolate this derivative.

The pitching moment due to elevator deflection is primarily due to the change in normal force of the horizontal tail due to elevator deflection:

$$C_{m_{\delta e}} = C_{z_{\delta e}} \, l_t \, / \, \bar{c} \qquad (41)$$

From Table 7, $C_{m_{\delta e}}$ should be approximately 3 times $C_{z_{\delta e}}$ for

5 - 3

the VRA; however, the present parameter estimates do not conform to this theoretical relationship.

The normal acceleration time histories from these runs initially show the effect of the erroneous C_{z_q} and $C_{z_{\delta e}}$. The estimated time history initial response to the elevator deflection is a visible acceleration opposite to the intended acceleration as seen in Figure 11. A pitch-up elevator deflection initially produced a large upward acceleration of the c.g. in the estimated time history (E). This response was clearly not evident in the measured normal acceleration (M).

Reference 3 and 10 suggest that the inverse of the second gradient of the cost function with respect to the unknown parameters, as calculated by the minimization algorithm, is a useful approximation to the parameter covariance matrix. Table 8 shows this matrix, normalized by the diagonal elements. The off-diagonal terms of this matrix are approximations to the correlation coefficients of corresponding parameters. The high correlation between $C_{z_{\delta e}}$ and $C_{m_{\delta e}}$ is expected from their geometric relationship. In addition, the aerodynamic bias estimates are highly correlated with the control derivatives possibly because of a bias in the trim elevator deflection measurement.

5 - 4
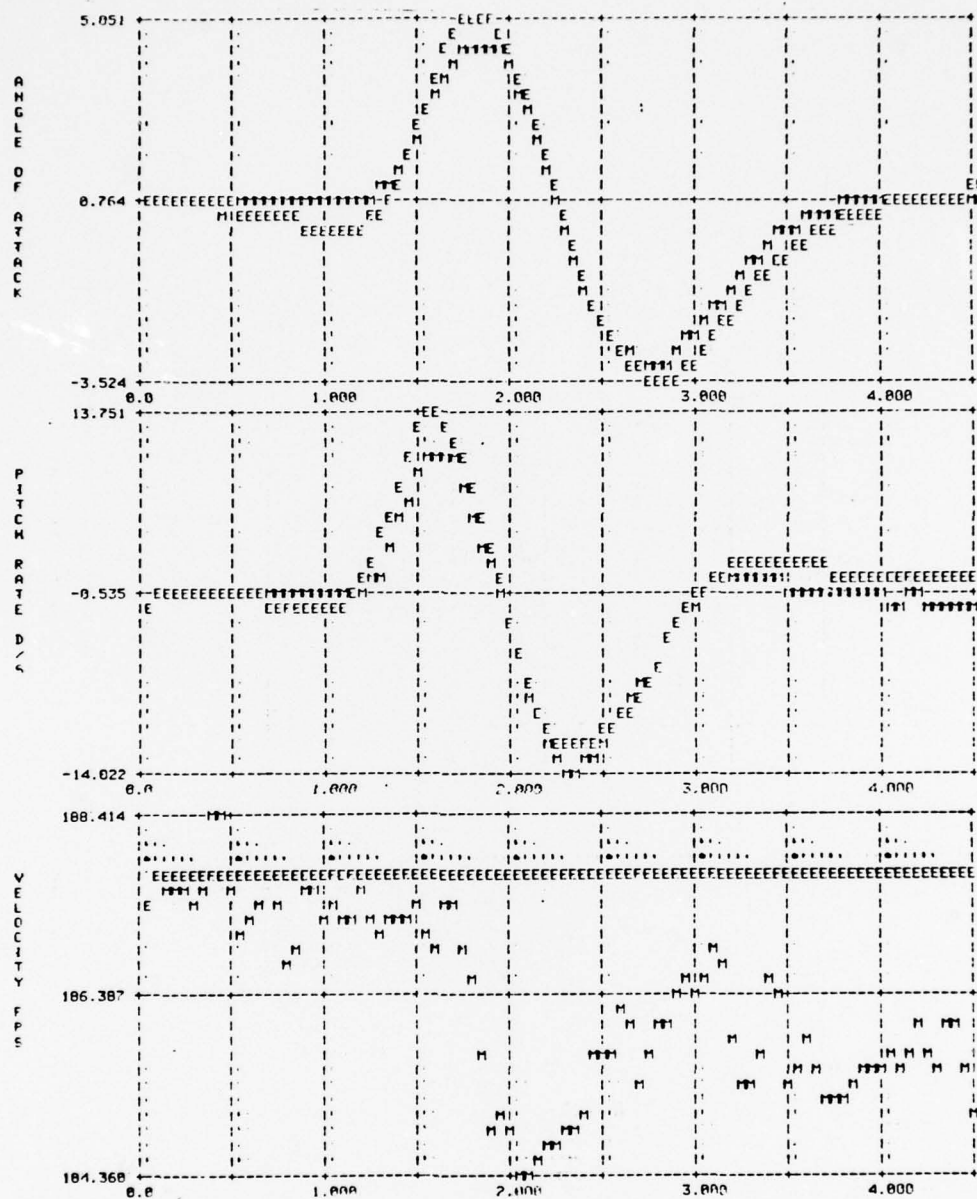
FIGURE 11. COMPARISON OF FLIGHT 2 DATA(M) WITH TIME HISTORIES(E) COMPUTED USING INITIAL ESTIMATES OF THE STABILITY AND CONTROL DERIVATIVES FOR AN ELEVATOR INPUT. (ABSCISSA IS TIME IN SEC)

5 - 5
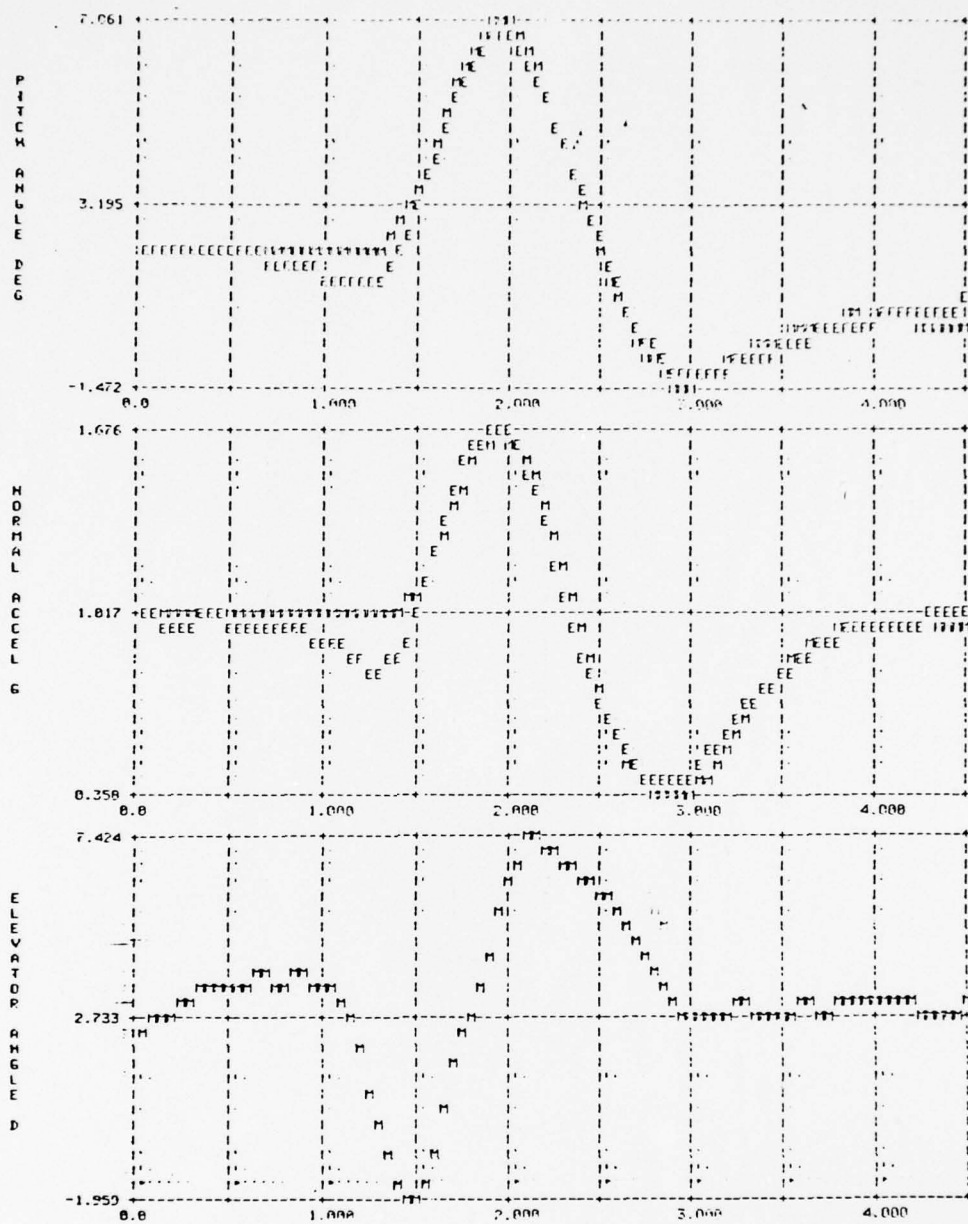
FIGURE 11. (CONTINUED).

TABLE 8. ESTIMATED LONGITUDINAL PARAMETER COVARIANCE MATRIX NORMALIZED BY THE DIAGONAL ELEMENTS.

	$Z_{\delta e}$	Z_o	Z_α	Z_q	$M_{\delta e}$	M_o	M_α	M_q	$\dot{\theta}_o$
$Z_{\delta e}$	1.	.97	.06	-.49	-.93	-.94	.10	.53	-.88
Z_o	.97	1.	.03	-.44	-.97	-.97	.11	.59	-.91
Z_α	.06	.03	1.	-.59	-.01	-.06	-.12	-.19	-.08
Z_q	-.49	-.44	-.59	1.	.40	.43	-.36	-.09	.52
$M_{\delta e}$	-.93	-.97	-.01	.40	1.	.99	-.09	-.66	.95
M_o	-.94	-.97	-.06	.43	.99	1.	-.06	-.59	.95
M_α	.10	.11	-.12	-.36	-.09	-.06	1.	.41	-.05
M_q	.53	.59	-.19	-.09	-.66	-.59	.41	1.	-.56
$\dot{\theta}_o$	-.88	-.91	-.08	.52	.95	.95	-.05	-.56	1.

5.2 Final Runs

The derivatives, Z_q and $Z_{\delta e}$, were held fixed at analog matching values ($C_{Z_q} = 0$; $C_{Z_{\delta e}} = -.2867$) since they were

5 - 7

not determinable from the data. In addition, the aerodynamic biases were calculated to balance the equations of motion initially and were held fixed during the estimation. The results of this second set of runs are summarized in Table 7. Note that the C_{Z_α} estimate increased in magnitude. The short-period mode damping derivative, C_{m_q} decreased in magnitude. $C_{m_{\delta e}}$ is now approximately three times the magnitude of $C_{Z_{\delta e}}$.

In attempting to reduce their standard deviations, the estimates were separated into sets by direction of initial elevator deflection. The variance in C_{m_α} and C_{m_q} decreased for the estimates separated in this way and all estimated derivatives had significantly different mean values based on this separation (see Appendix B). This nonlinear response to elevator inputs again suggests that the analytical model should be reexamined and revised. It also suggests that smaller amplitude inputs must be used to remain within the linear range of aircraft response. The penalty of poorer signal-to-noise ratios on the quality of estimates dictates that the measurement noise must be reduced to maintain high signal-to-noise ratios.

Use of a Kalman filter/smoother during data processing is one approach to reducing noise in the data provided by

5 - 8

the VRA's existing sensors. Care must be exercised in this procedure to prevent parameter estimates from being biased by the dynamic model assumed for the Kalman filter/smoother. A long-term approach to noise reduction is the replacement of the hardware used for data processing in this study with equipment better suited for digital data analysis.

Table 9 compares the estimates derived in this study with analog matching results and published estimates for the Navion in different configurations. C_{Z_α} is higher than expected from earlier results. Reference 3 suggests that failure to include C_{Z_q} in the analytical model results in a larger amplitude C_{Z_α} estimate. The results from the initial runs suggest that a positive C_{Z_q} is required to reduce C_{Z_α} estimates from the given data. Additional runs including C_{Z_q} in the model resulted in increased magnitude C_{Z_α} estimates for negative C_{Z_q} estimates. The variance in the C_{Z_q} estimates still was very high. Additional data would better determine the relationship of C_{Z_q} and C_{Z_α}.

The three estimated moment derivatives have magnitudes smaller than the analog matching results, however, they are within one standard deviation of those results, with the exception of C_{m_q}, which is half the analog value. The $C_{m_{\delta e}}$ estimate is approximately three times the $C_{Z_{\delta e}}$ estimate.

5 - 9

TABLE 9. COMPARISON OF LONGITUDINAL DERIVATIVE ESTIMATES
WITH ANALOG MATCHING AND PUBLISHED RESULTS.

		Analog Match	Ref.3	Ref.2	Ref.1	Ref.18
C_{z_α}	-5.623	-4.588	-4.3/-4.9	-6.0/-6.4	-4.5/-4.5	-4.4/----
C_{z_q}	C.0	0.0	-15.9/-27.1			
$C_{z_{\delta e}}$	-.2867	-.2867	-.51/-.52	----/----	-.43/-.53	-.355/----
C_{m_α}	-.6107	-.6412	-.77/-.84	----/----	-.95/----	----/----
C_{m_q}	-7.867	-14.41	-24.6/-22.4	-18.3/-15.5	----/----	-14.3/----
$C_{m_{\delta e}}$	-.8207	-.9599	-1.4/-1.5	-1.4/-1.5	-1.4/-1.5	----/----

Additional data using improved elevator input shapes
and flap deflections could reduce the correlation of several
of the derivatives. An improved estimation method also is
needed to reduce the biases in estimates resulting from
holding elements of correlated sets of derivatives fixed.

Time history matches using the stability and control
derivatives estimated in this study show good agreement. In

5 -10
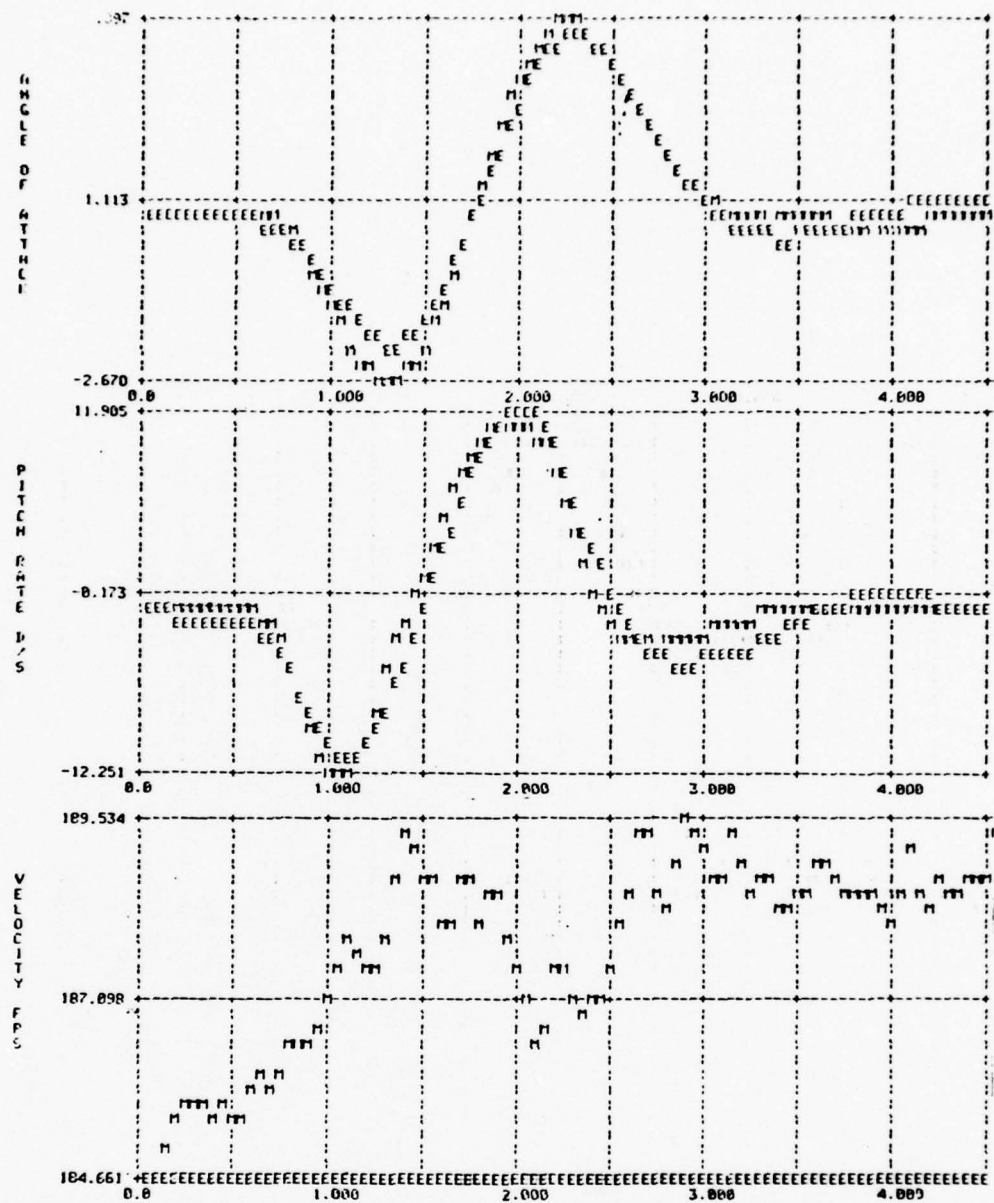
FIGURE 12. COMPARISON OF FLIGHT 1 DATA(M) WITH TIME
HISTORIES(E) COMPUTED USING THE PRESENT STUDY STABILITY AND
CONTROL DERIVATIVES FOR AN ELEVATOR DOUBLET INPUT.
(ABSCISSA IS TIME IN SEC)

5 - 11
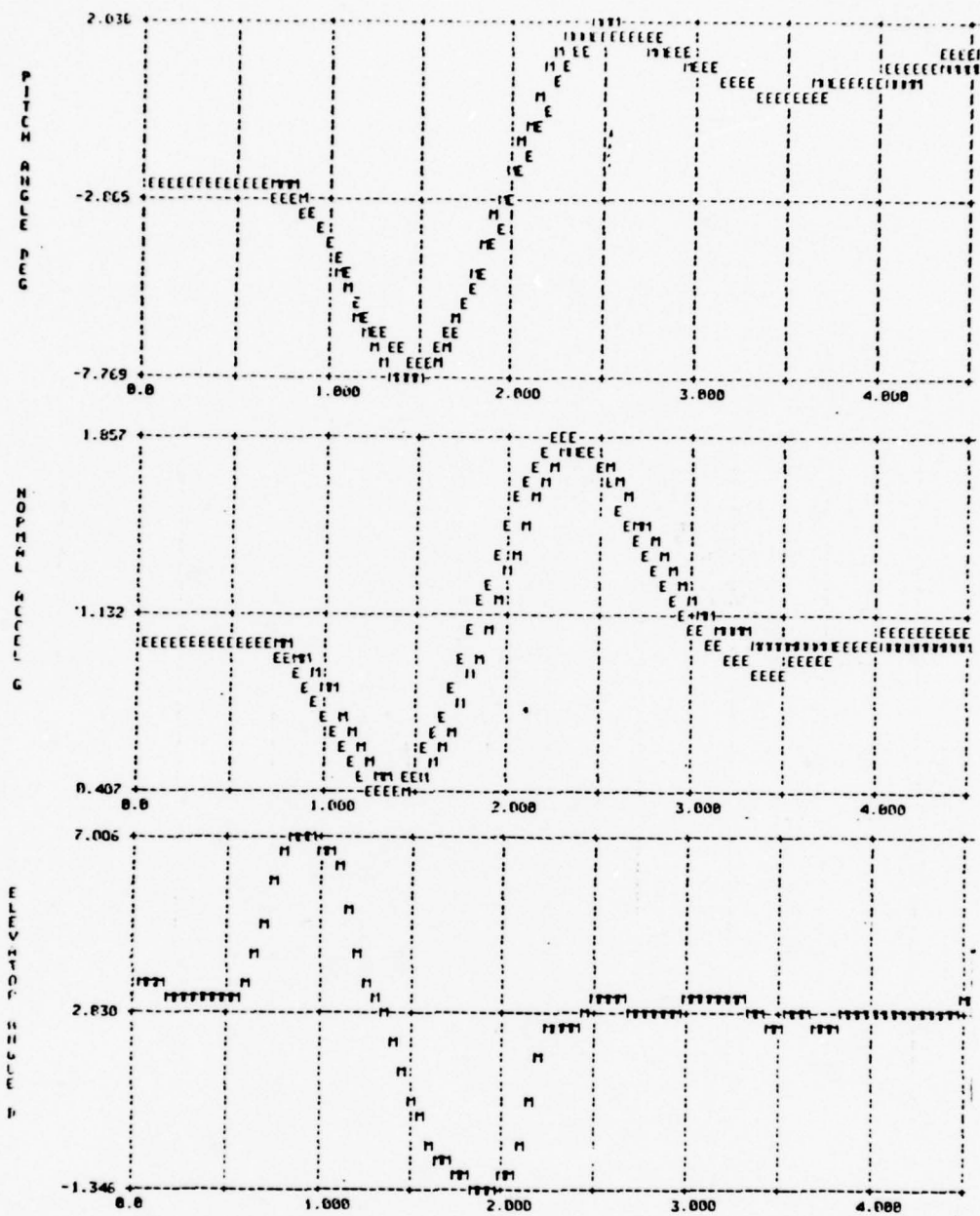
FIGURE 12. (CONTINUED).

5 -12

Figure 12, the angle-of-attack matching and the normal acceleration matching do suggest some inconsistency in the measurements. While the estimated time history tends to undershoot extrema in the angle-of-attack measurements, it tends to overshoot extrema in the normal acceleration measurements. This demonstrates the effectiveness of the minimization algorithm, as well as the adverse effects of scale factor and bias errors in the measurements. An error in the upwash correction factor of the angle-of-attack measurements might result in the inconsistency between measurements sources.

It was suggested that an error in the upwash correction for angle-of-attack measurements also might result in a C_{z_q} estimate with large variance. Six additional runs were made using two elevator doublet input time histories (Appendix B). These runs included C_{z_q} in the model and varied the upwash correction factor from 1 (no correction) to 1.9. The results suggest that there is a strong relationship between the upwash correction and C_{z_q} but that the variance in the C_{z_q} estimate is not reduced, as seen in Figure 13. While some matches improved, the undershoot-overshoot relationship was never reversed (α measurements were consistently undershot by α estimates).

5 -13
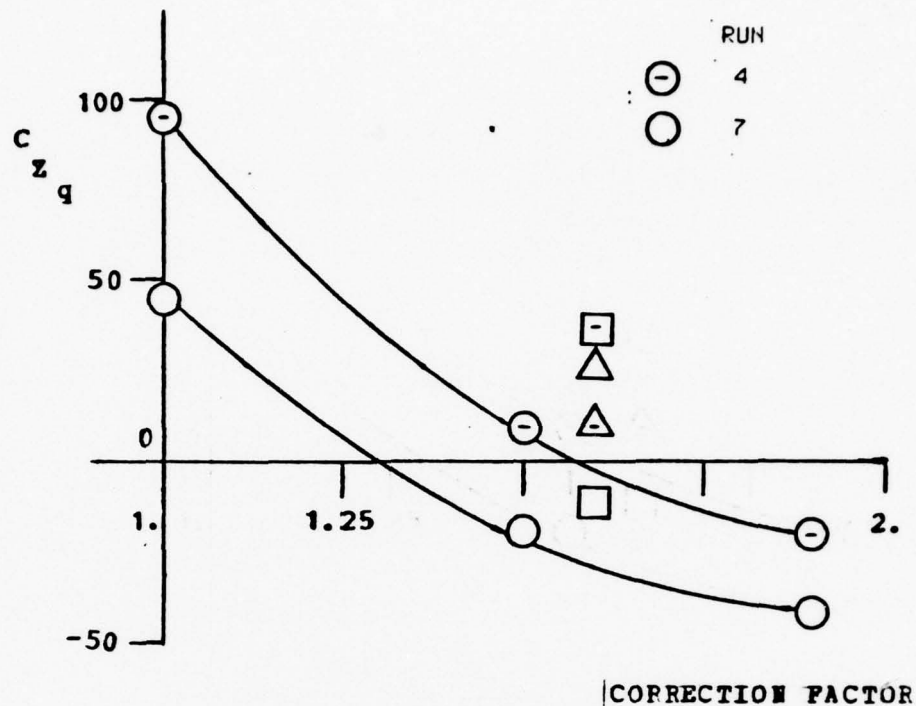
FIGURE 13. THE RELATIONSHIP BETWEEN ANGLE-OF-ATTACK UPWASH CORRECTION FACTOR AND THE COEFFICIENT FOR THE RATE OF CHANGE OF NORMAL FORCE WITH RESPECT TO PITCH RATE FOR TWO FLIGHT 1 ELEVATOR INPUT TIME HISTORIES.

     Aerodynamic biases were held fixed during these runs. The four data points at a correction factor of 1.6 show that failure to use the correct analytical model results in biased estimates. Two of the data points (triangles) are the estimates from initial runs for these time histories. Here Z_q, $Z_{\delta e}$, and the aerodynamic biases were estimated as well as the other short period mode derivatives. The other

5 - 14

two points (squares) were estimated with the aerodynamic biases and $Z_{\delta e}$ being fixed. This result clearly indicates the need for further research on the analytical model.

Additional runs were made to determine the effects of a non-zero pitching moment with respect to rate of change of angle of attack ($C_{m_{\dot\alpha}}$). This term was introduced using the acceleration transformation matrix, R:

$$R\,\dot{\underline{x}} = A\,\underline{x} + B\,\underline{u} \qquad\qquad (42)$$

Inverting R and premultiplying the A and B matrices correctly accounts for the unsteady aerodynamic effect on the stability and control derivatives of this term. $C_{m_{\dot\alpha}}$ was set at -4.385, the value from analog matching results. This $C_{m_{\dot\alpha}}$ increased $C_{m_q} + C_{m_{\dot\alpha}}$ by 25 percent and increased $C_{m_{\delta e}}$ by 10 percent towards the analog matching results. A similar result is reported in Ref 3. C_{m_α} changed by less than 2 percent from its previously estimated value.

5.3 Conclusions

Initial estimates demonstrated the dynamic velocity error and the small velocity perturbation response to elevator

5 -15

doublet input time histories of 5-sec. In addition, physically nonrealizable estimates of certain derivatives and prediction of high correlations in pairs of estimates suggested that the associated derivatives should be held fixed during estimation. These runs produced good time history matches and fair comparisons with previous work. Separation of results by initial deflection reduced the variance in some estimates and clearly indicated a nonlinear aircraft response. This recommends further refinement of the analytical model to include nonlinear terms and use of lower amplitude elevator inputs to stay within the linear range of the lift curve slope. This in turn requires reducing measurement noise either by smoothing existing data or by employing improved sensors. The effects of scale factor errors in angle-of-attack measurements were investigated, and the results indicate that further verification of the upwash correction should be made. In addition, an improved method for estimating highly correlated derivatives must be devised. Inclusion of a fixed value of $C_{m_{\alpha}}$ seemed to improve moment derivative estimates and should be estimated. This again would require modification of the analytical model.

6. CONCLUSIONS AND RECOMMENDATIONS

The research for this thesis resulted in several conclusions and recommendations about analytical models, data collection and derivative estimation:

.   The absense of measurement and process noise in the flight data is not always a reasonable assumption, as the quality of estimates is directly related to the validity of this assumption.

.   Instrument errors result in the degradation of the quality of derivative estimates. The aircraft static ports, angle-of-attack and sideslip vanes, and lateral accelerometer should be studied to determine the effects of high frequency inputs, rapid changes in air flow, and upwash effects.

.   Calibration procedures should be reexamined with the aim of reducing human error. Simple calibration instruments can be constructed that result in consistent results.

.   Improved control input designs can now be verified using the VRA digital flight control system, which is capable of generating repeatable inputs of arbitrary pulse (or wave) shape.

6 - 1

.   The replacement of analog-to-digital conversion hardware with equipment better suited to digital data analysis will reduce measurement noise and biases added by the multitude of components now used.

.   Mass and inertia information must be determined for the VRA in its current configuration. The effects of inertia coupling should be documented prior to identifying aerodynamic coupling parameters.

.   Poor signal-to-noise ratios aggravated by failure to sufficiently excite all modes of motion result in poor quality derivative estimates. These effects are visible in the time history matches produced.

.   The nonlinear response in roll, pitch,and yaw to control estimates is documented by the reduction in variance of estimates separated by initial deflection of the control surface. This suggests that the assumptions used in deriving the analytical model must be reexamined and additional effects must be modelled in the equations.

.   Cramer-Rao lower bounds to the standard deviations in estimates are reasonable confidence level indicators,although they rarely reflect true standard deviations.

6 - 2

. An improved method for estimating highly correlated derivatives must be devised. Improved control input design is a fruitful direction for research.

. Nonphysically realizable estimates of derivatives can cause obvious errors in time history matches that are not corrected by the minimization algorithm. Measurement and process noise can account for these estimates as well as poor excitation of modes of motion.

. Good time history matches do not guarantee good parameter estimates in the presence of measurement and process noise. Modeling errors and noise and biases in the instruments degrade the quality of estimates.

Further research is needed on the aircraft analytical model and minimization algorithm. Instrument studies should precede further estimation research. Input design studies offer improved quality of estimates even with current measurement and process noise problems.

6 - 3

APPENDIX A

TABULATED LATERAL-DIRECTIONAL DERIVATIVE
ESTIMATES

The Modified Maximum Likelihood Estimation program used
in this study produces estimates of stability and control
derivatives and lower bounds to the standard deviations of
the estimates (Cramèr-Rao bounds). Table 10 lists the
lateral-directional derivative estimates and Cramèr-Rao
bounds for the twenty time histories discussed in Chapter 4.
Zero values for the Cramèr-Rao bounds indicate that these
derivatives were held fixed at an assigned value. Mean
values and standard deviations are also listed.

Runs 1 through 7 in Table 10, are estimates from
aileron pulse input time histories for Flight 1. Taken
together, the standard deviations of all stability
derivatives and aileron control derivatives are reduced from
values for all estimates. Standard deviations are reduced
further for several derivatives by grouping estimates into
sets according to direction of aileron deflection as in
Table 11 (3 positive and 4 negative inputs). This reduction
in variance indicates a nonlinear response of the VRA to
aileron inputs.

A - 1

CY DERIVATIVES

RUN	BETA	P		R	DA	DR	DSF
1	-0.55264+0.10234	0.0000+	0.012	0.00000+0.00000	0.03360+0.03612	0.06801+0.27352	0.07096+0.20344
2	-0.60792+0.03162	0.0000+	0.007	0.00000+0.00000	0.02164+0.00837	0.06536+0.09840	0.45026+0.05011
3	-0.54399+0.07426	0.0000+	0.006	0.00000+0.00000	0.06014+0.01930	0.16017+0.14202	0.54187+0.12574
4	-0.85665+0.09427	0.0000+	0.009	0.00000+0.00000	0.03078+0.02676	0.44411+0.44155	0.24936+0.17841
5	-0.86181+0.03469	0.0000+	0.005	0.00000+0.00000	-0.00590+0.00753	0.24947+0.13051	0.17954+0.07804
6	-0.96169+0.04962	0.0000+	0.005	0.00000+0.00000	-0.00861+0.00739	0.13317+0.08140	0.47780+0.06172
7	-1.07234+0.07401	0.0000+	0.006	0.00000+0.00000	0.02483+0.01128	0.32850+0.09545	0.30597+0.05955
8	-0.86462+0.01288	0.0000+	0.000	0.00000+0.00000	0.01465+0.00000	0.37654+0.01564	0.45936+0.10455
9	-0.89338+0.01927	0.0000+	0.000	0.00000+0.00000	0.01441+0.00000	0.35441+0.02346	0.06870+0.10524
10	-0.74158+0.01594	0.0000+	0.000	0.00000+0.00000	0.01465+0.00000	0.40428+0.01787	0.73425+0.09816
11	-1.00432+0.02235	0.0000+	0.000	0.00000+0.00000	-0.06516+0.17876	0.31842+0.03023	0.36985+0.16395
12	-1.37202+0.24500	0.0000+	0.000	0.00000+0.00000	0.01470+0.00000	0.38185+0.00000	0.55181+0.02380
13	-0.55117+0.13981	0.0000+	0.000	0.00000+0.00000	0.01505+0.00000	0.39090+0.00000	0.39252+0.01623
14	-1.08202+0.12156	0.0000+	0.000	0.00000+0.00000	0.01520+0.00000	0.39361+0.00000	0.40565+0.01447
15	-1.20014+0.08001	0.0000+	0.000	0.00000+0.00000	0.09461+0.11881	0.42203+0.79174	0.60708+0.02912
16	-1.68025+0.31163	0.0000+	0.000	0.00000+0.00000	0.04893+0.77748	0.29171+1.04352	0.42164+0.09029
17	-0.55604+0.19105	0.0000+	0.000	0.00000+0.00000	1.04593+0.25380	0.27519+0.65798	0.59277+0.04619
18	-1.44839+0.10002	0.0000+	0.000	0.00000+0.00000	-0.42680+0.27140	0.41564+0.71994	0.63177+0.04303
19	-1.07371+0.17399	0.0000+	0.000	0.00000+0.00000	0.02631+0.40074	0.39208+0.92943	0.70214+0.08203
20	-0.96818+0.26953	0.0000+	0.000	0.00000+0.00000	0.26393+1.02336	0.41977+2.75043	0.54831+0.13504

MEAN AND STD DEV BASED ON 20 SAMPLES

	BETA	P		R	DA	DR	DSF
20	-0.94464+0.30801	0.0000+	0.000	0.00000+0.00000	0.05926+0.25499	0.17262+0.28732	0.09112+0.46675
	32.6%	0.0%	0.0%	0.0%	430.3%	166.5%	512.2%

A - 2

TABLE 10. LATERAL-DIRECTIONAL DERIVATIVE ESTIMATES AND THEIR CRAMER-RAO BOUNDS.

CL DERIVATIVES

RUN	BETA	P	R	DA	DR	DSF
1-	-0.0963+0.00931	-0.5460+ 0.014	0.24389+0.03128	-0.10935+0.00465	-0.05415+0.02425	0.05707+0.01836
2-	-0.0168+0.00572	-0.6597+ 0.017	0.02296+0.02186	-0.22089+0.00517	-0.04022+0.02054	0.03639+0.00969
3-	-0.0707+0.00736	-0.5997+ 0.015	0.17435+0.03056	-0.20393+0.00406	-0.02246+0.01493	0.11449+0.01959
4-	-0.0781+0.00613	-0.5480+ 0.014	0.09726+0.03343	-0.16136+0.00358	-0.02716+0.03190	-0.02876+0.01175
5-	-0.1055+0.00427	-0.5246+ 0.012	0.06461+0.01591	-0.15631+0.00316	-0.08538+0.02027	0.08675+0.01400
6-	-0.0733+0.00497	-0.5503+ 0.012	0.04175+0.03423	-0.16399+0.00298	-0.01547+0.01380	-0.02567+0.01367
7-	-0.1096+0.00826	-0.4976+ 0.011	0.05745+0.02169	-0.16617+0.00349	-0.02057+0.01318	0.02813+0.00763
8-	-0.1116+0.00967	-0.6251+ 0.056	0.08943+0.01077	-0.18892+0.00000	0.02395+0.00211	0.14657+0.01068
9-	-0.0760+0.00528	-0.4243+ 0.027	0.12485+0.00706	-0.18170+0.00000	0.02300+0.00200	0.08274+0.00810
10-	-0.1586+0.00028	-0.8191+ 0.050	0.09411+0.01103	-0.18863+0.00000	0.02653+0.00356	0.06601+0.01174
11-	-0.1184+0.03466	-0.6819+ 0.208	0.12692+0.02055	-0.16159+0.03444	0.02430+0.00441	0.16520+0.05487
12-	-0.1792+0.01972	-0.4782+ 0.015	0.16622+0.08092	-0.19012+0.00000	0.02498+0.00000	0.01891+0.00370
13-	-0.0827+0.01956	-0.7945+ 0.113	0.13592+0.04522	-0.19923+0.00000	0.02619+0.00000	-0.00006+0.00264
14-	-0.1414+0.02035	-0.7847+ 0.115	0.05393+0.04415	-0.20198+0.00000	0.02653+0.00000	-0.00212+0.00232
15-	-0.1093+0.05441	-0.4916+ 0.202	0.27588+0.06549	-0.13053+0.03259	0.02395+0.16382	-0.01942+0.00637
16-	-0.0945+0.01203	-0.2264+ 0.051	0.34088+0.03693	-0.09128+0.02101	0.02401+0.02740	-0.01243+0.00287
17-	-0.0702+0.02361	-0.4635+ 0.123	0.19699+0.05242	-0.14686+0.03523	0.02487+0.03004	-0.00539+0.00244
18-	-0.0591+0.03234	-0.6909+ 0.372	0.02906+0.07885	-0.15952+0.06412	0.02682+0.12010	0.00567+0.04510
19-	-0.1245+0.04985	-0.7305+ 0.302	0.03414+0.04148	-0.11133+0.05919	0.02418+0.07558	0.05323+0.01012
20-	-0.1260+0.11122	-0.7345+ 0.594	0.03565+0.12050	-0.12251+0.10641	0.02550+0.19465	0.01329+0.01485

MEAN AND STD DEV BASED ON 20 SAMPLES

| | -0.0981+0.02853 | -0.5936+ 0.144 | 0.10629+0.10127 | -0.16731+0.03321 | 0.00297+0.03294 | 0.04123+0.05227 |
| | 29.1% | 24.2% | 95.3% | 19.9% | *****% | 128.0% |

A - 3

TABLE 10. (continued).

CN DERIVATIVES

RUN	BETA	P	R	DA	DR	DSF
1	0.07644+0.00621	-0.0870+0.010	-0.11029+0.02382	-0.02235+0.00319	-0.00189+0.01621	0.01616+0.01377
2	0.07952+0.00224	-0.0925+0.007	-0.10814+0.00647	-0.02143+0.00231	-0.00625+0.00764	0.01278+0.00417
3	0.08446+0.00398	-0.0700+0.006	-0.12562+0.01056	-0.01570+0.00184	-0.08257+0.00714	0.00923+0.00783
4	0.07243+0.00362	-0.0584+0.009	-0.11557+0.01554	-0.00796+0.00272	-0.06188+0.01701	0.01278+0.00688
5	0.08922+0.00258	-0.1265+0.006	-0.12126+0.00748	-0.02273+0.00177	-0.06146+0.01137	0.02172+0.00704
6	0.08647+0.00385	-0.0914+0.005	-0.17747+0.01485	-0.01874+0.00149	-0.02556+0.00580	0.03954+0.00578
7	0.12319+0.00736	-0.0797+0.006	-0.08949+0.00904	-0.02395+0.00210	-0.02567+0.00547	0.03684+0.00407
8	0.09185+0.00378	-0.0658+0.022	-0.12806+0.00351	-0.01811+0.00000	-0.10062+0.00102	0.04928+0.00437
9	0.08561+0.00427	-0.1060+0.023	-0.14719+0.00361	-0.01742+0.00000	-0.09793+0.00117	0.01725+0.00653
10	0.05151+0.00358	-0.2929+0.021	-0.19088+0.00532	-0.01811+0.00000	-0.10005+0.00166	0.00097+0.00595
11	0.07088+0.03330	-0.2414+0.201	-0.15629+0.01762	-0.01656+0.03032	-0.09025+0.00344	0.02189+0.05239
12	0.07787+0.00836	-0.1155+0.010	-0.37345+0.05182	-0.01822+0.00000	-0.10154+0.00000	0.04365+0.00281
13	0.08773+0.01200	-0.1408+0.076	-0.14213+0.01570	-0.01908+0.00000	-0.10641+0.00000	0.03667+0.00157
14	0.05994+0.01078	-0.1419+0.065	-0.13473+0.01573	-0.01937+0.00000	-0.10784+0.00000	0.04406+0.00104
15	0.07220+0.01752	-0.1954+0.063	-0.18207+0.02330	-0.03295+0.00000	-0.09896+0.05507	0.05191+0.00228
16	0.05912+0.01135	-0.3806+0.055	-0.11516+0.03483	-0.00997+0.01968	-0.10159+0.02483	0.02923+0.00234
17	0.07856+0.00028	-0.1060+0.046	-0.11978+0.02221	-0.05810+0.01291	-0.09105+0.01125	0.03856+0.00096
18	0.09413+0.02864	-0.3099+0.332	-0.12368+0.07385	-0.01163+0.05449	-0.11208+0.11059	0.04630+0.00455
19	0.11695+0.02138	-0.0369+0.128	-0.11227+0.01642	-0.01759+0.02576	-0.09861+0.02562	0.04475+0.00453
20	0.11999+0.05361	-0.0243+0.291	-0.14802+0.06230	-0.03679+0.04654	-0.10537+0.06962	0.04870+0.04872

MEAN AND STD DEV BASED ON 20 SAMPLES

	BETA	P	R	DA	DR	DSF
20	0.08357+0.01867	-0.1381+0.095	-0.13456+0.08136	-0.02159+0.01074	-0.06038+0.06006	0.02412+0.02530
	22.3%	68.4%	60.5%	49.7%	99.5%	104.9%

A - 4

TABLE 10. (concluded).

AILERON PULSE INPUT

	P	P	DA	DR	DSF

CY DERIVATIVES
FOR METH

MEAN AND STD DEV BASED ON   5 SAMPLES
3 -0.56813+0.09833 0.00000 0.00000+0.00000 0.04013+0.01576-0.05427+0.09258+0.35436+0.20336
                      0.0%   39.3%   170.6%   57.5%

MEAN AND STD DEV BASED ON   4 SAMPLES
4 -0.73312+0.08888 0.00000 0.00000+0.00000 0.01028+0.01768-0.09749+0.29457-0.30329+0.11025
                      0.0%   172.0%   302.2%   36.4%

CL DERIVATIVES

MEAN AND STD DEV BASED ON   5 SAMPLES
3 -0.08803+0.01017 -0.00184 0.046 0.17040+0.06168 -0.20806+0.09927 0.03894+0.01297 0.06931+0.03304
          12.0%   7.0%   36.2%   4.5%   33.3%   47.7%

MEAN AND STD DEV BASED ON   4 SAMPLES
4 -0.09315+0.00118 -0.05014+   0.021 0.00623+0.00021 -0.16195+0.05714+0.00368-0.03714+0.02815 0.02795+0.04086
          12.0%   31.0%   2.3%   75.8%   146.2%

CN DERIVATIVES

MEAN AND STD DEV BASED ON   5 SAMPLES
3 -0.02881+0.00007 0.08822+ 0.010-0.114 0.00778 -0.01985+0.00291-0.02607+0.04004 0.00657+0.01125   ---
           6.1%   11.5%   6.8%   14.8%   155.8%   171.5%

MEAN AND STD DEV BASED ON   4 SAMPLES
4 -0.02880+0.06803 -0.06800   0.055-0.1 0.00740+0.03207 -0.01960+0.00714 0.00020+0.03631 0.02133+0.02083
                                        3.5%   37.9%   ******   97.7%

TABLE 11.   MEANS AND STANDARD DEVIATIONS FOR LATERAL DIRECTIONAL DERIVATIVE ESTIMATES SEPARATED BY CONTROL INPUT INITIAL DIRECTION. (STANDARD DEVIATION AS A PERCENTAGE OF THE MEAN LISTED BELOW STANDARD DEVIATION)

A - 5

RUDDER DOUBLET INPUT

CY DERIVATIVES

RUN	BETA	$\dot{P}$	R	DA	DR	DSF

MEAN AND STD DEV BASED ON   2 SAMPLES
2-0.37295+0.13137 0.0000+ 0.000 0.00000+0.00000 -0.02525+0.03991 0.36135+0.04293-0.18220+0.55205
       15.0%   0.0%   0.0%   158.0%   11.9%   303.0%

MEAN AND STD DEV BASED ON -2 SAMPLES
2-0.87900+0.01439 0.0000+ 0.000 0.00000+0.00000 0.01453+0.00012 0.36548+0.01106-0.19533+0.26403
       1.6%   0.0%   0.0%   0.8%   3.0%   135.2%

CL DERIVATIVES

MEAN AND STD DEV BASED ON   2 SAMPLES
2-0.12735+0.00951 -0.7505+ 0.069 0.11052+0.01640 -0.17511+0.01352 0.02541+0.00112 0.11560+0.04959
       6.7%   9.1%   14.8%   7.7%   4.4%   42.9%

MEAN AND STD DEV BASED ON   2 SAMPLES
2-0.02360+0.01756 -0.5247+ 0.100 0.10714+0.01771 -0.10531+0.00360 0.02352+0.00043 0.11466+0.03192
       18.8%   19.1%   16.5%   1.9%   1.8%   27.8%

CN DERIVATIVES

MEAN AND STD DEV BASED ON   2 SAMPLES
2 0.06120+0.00968 -0.2672+ 0.026-0.17359+0.01729 -0.01733+0.00077-0.09515+0.00490 0.01046+0.01143
       15.8%   9.6%   10.0%   4.5%   5.1%   109.3%

MEAN AND STD DEV BASED ON   2 SAMPLES
2 0.08873+0.00312 -0.0859+ 0.020-0.13762+0.00957 -0.01776+0.00034-0.09927+0.00134-0.01602+0.03326
       3.5%   23.4%   7.0%   1.9%   1.4%   207.7%

A - 6

TABLE 11. (continued).

SIDE FORCE SURFACE INPUT

CY DERIVATIVES

RUN	BETA	P	R	DA	DR	DSF

MEAN AND STD DEV BASED ON 2 SAMPLES
2 -1.02095+0.05276 0.0000+0.00000+0.00000 0.11081+0.14512 0.40592+0.01385 0.62523+0.07691
      5.2%   0.0%   122.1%   3.4%   12.3%

MEAN AND STD DEV BASED ON 4 SAMPLES
4 -1.22120+0.41989 0.0000+0.00000+0.00000 0.19067+0.53433 0.14332+0.32769 0.56331+0.06298
      34.4%   0.0%   280.2%   228.6%   14.7%

CL DERIVATIVES

MEAN AND STD DEV BASED ON 2 SAMPLES
2 -0.12423+0.00178 -0.7325+0.002 0.03490+0.00076 -0.11692+0.00559 0.02484+0.00066 0.02326+0.00997
      1.4%   0.3%   2.2%   4.8%   2.7%   42.9%

MEAN AND STD DEV BASED ON 4 SAMPLES
4 -0.06963+0.03261 -0.4681+0.165 0.19617+0.13967 -0.13205+0.02568 0.02491+0.00116 -0.00579+0.01060
      46.8%   35.2%   71.2%   19.5%   4.7%   183.1%

CN DERIVATIVES

MEAN AND STD DEV BASED ON 2 SAMPLES
2 0.11847+0.00152 -0.0306+0.006 -0.13015+0.01787 -0.02719+0.00960 -0.10199+0.00338 0.04673+0.00198
      1.3%   20.7%   13.7%   35.3%   3.3%   4.2%

MEAN AND STD DEV BASED ON 4 SAMPLES
4 0.07532+0.01163 -0.2480+0.105 -0.07759+0.11399 -0.02816+0.01952 -0.05539+0.08469 0.04141+0.00838
      15.4%   42.5%   146.9%   69.3%   152.9%   20.2%

TABLE 11. (concluded).

Runs 8 through 11 in Table 10 are estimates from rudder doublet input time histories for Flight 1. Again standard deviations are reduced for all stability derivatives and the quality of rudder derivative estimates is much improved as expected. Table 11 shows that, as with aileron inputs, variances are reduced for some derivatives when separated according to initial rudder deflection (2 positive, 2 negative). This evidence of nonlinear response suggests that further research of the analytical model is needed.

Runs 12 through 15 in Table 10 are estimates from side-force surface input time histories for Flight 1. Because of a side-force-surface-to-aileron interconnect and a side-force-surface-to-rudder interconnect used on this flight to better simulate pure lateral translations, side-force surface control derivatives were estimated holding the aileron and rudder derivatives fixed at previously estimated values.

Runs 16 through 20 in Table 10 are estimates from side-force surface input time histories for Flight 2. No control interconnects were used on this flight. The single positive and two negative side-force surface pulses (15, 19, and 20) produced larger state perturbations (and thus higher signal to noise ratios) than did the single positive and two

A - 8

negative doublets (16, 17, and 18). Cramer-Rao bounds for both types of inputs are similar however. Table 11 separates estimates by direction of initial input and again the variance in some derivatives is reduced.

Chapter 4 discusses the questionable $C_{n_{\delta a}}$ derivative estimate. The estimate is 5 times as large as the analog matching result and is opposite in sign. Table 12 lists the estimates from two aileron pulse time histories where aileron control derivatives were fixed at analog matching values. In comparing the estimates with those for runs 1 and 4 from Table 10, C_{l_β}, C_{l_r}, C_{n_β}, and C_{n_r} estimates doubled in magnitude although C_{n_p} did decrease towards the analog matching result.

CY DERIVATIVES
RUN BETA   P   R   DA   DR   DSF
1 -1.30615+0.15223 0.0016+ 0.09662.46434+1.00548 0.00000+0.00000 0.36340+0.00000 0.58370+0.00000
2 -0.30557+0.17937 -0.4574+ 0.08865.98349+0.70767 0.00000+0.00000 0.36340+0.00000 0.58370+0.00000

MEAN AND STD DEV BASED ON 2 SAMPLES
2 -0.80586+0.50029 -0.2279+ 0.23064.22391+1.76002 0.00000+0.00000 0.36340+0.00024 0.58370+0.00065
                 62.1%   100.7%   0.0%   0.1%   0.1%

CL DERIVATIVES
1 -0.13939+0.01897 -0.5485+ 0.009 0.15687+0.03469 -0.15760+0.00000 0.02460+0.00000 0.00000+0.00000
2 -0.26661+0.04254 -0.4287+ 0.011 0.23650+0.05660 -0.15760+0.00000 0.02460+0.00000 0.00000+0.00000

MEAN AND STD DEV BASED ON 2 SAMPLES
2 -0.20300+0.06361 -0.4886+ 0.060 0.19668+0.03982 -0.15760+0.00012 0.02460+0.00000 0.00000+0.00000
                 31.3%   12.3%   0.1%   0.0%   0.0%

CN DERIVATIVES
1 0.12254+0.01240 -0.0555+ 0.003-0.23368+0.01586 0.00390+0.00000 -0.09740+0.00000 0.04300+0.00000
2 0.24158+0.03382 -0.0806+ 0.006-0.39118+0.02571 0.00390+0.00000 -0.09740+0.00000 0.04300+0.00000

MEAN AND STD DEV BASED ON 2 SAMPLES
2 0.18206+0.05952 -0.0680+ 0.013-0.31243+0.07875 0.00390+0.00000 -0.09740+0.00000 0.04300+0.00004
                 32.7%   18.5%   0.0%   0.0%   0.1%

TABLE 12. DERIVATIVE ESTIMATES FOR RUNS HOLDING $C_{n_{\delta a}}$ FIXED AT .

THE ANALOG MATCHING RESULT.

APPENDIX B

TABULATED LONGITUDINAL DERIVATIVE ESTIMATES

Longitudinal stability and control derivatives were identified by the Modified Maximum Likelihood Estimation program using elevator doublet input time histories from Flight 2. Table 13 lists the estimates and lower bounds to the standard deviations (Cramer-Rao bounds) for initial runs using 4 negative initial input doublets (runs 1 through 4) and 3 positive initial input doublets (runs 5 through 7). Listed also are the averages and standard deviations for all 7 runs, the negative runs and the positive runs.

Table 14 lists the estimates from 2 time histories (4 and 7) for varying angle of attack upwash correction factors. Angle of attack measurements were divided by correction factors of 1, 1.5, and 1.9. C_{z_q} appears to be the most sensitive of all estimated derivatives to errors in the upwash correction. The variance in C_{z_q} is not reduced however by changing upwash correction factor.

```
CZ DERIVATIVES
RUN ALPHA               Q                   DE
  1-3.28187+0.15433 20.1563+  8.956,-0.82853+0.08952
  2-3.66989+0.14645  4.1088+  6.858 -1.11753+0.10091
  3-4.07454+0.15917  2.2472+  6.158 -1.68999+0.14265
  4-3.80012+0.12230  9.2276+  4.883 -1.11669+0.08668
  5-3.86492+0.13668 19.7470+  6.482 -1.40569+0.09275
  6-3.28039+0.13495 54.5444+  8.528 -0.66660+0.09959
  7-3.62405+0.08399 22.5053+  4.218 -1.22202+0.06589

MEAN AND STD DEV BASED ON   7 SAMPLES
  7-3.65654+0.27307 18.9338+ 16.368 -1.14958+0.31653
            7.5%             86.5%            27.5%

MEAN AND STD DEV BASED ON-  4 SAMPLES
  4-3.70660+0.28542  8.9350+  6.965 -1.18818+0.31275
            7.7%             77.9%            26.3%

MEAN AND STD DEV BASED ON +  3 SAMPLES
  3-3.58979+0.23984 32.2656+ 15.794 -1.09810+0.31420
            6.7%             48.9%            28.6%



CM DERIVATIVES
RUN ALPHA               Q                   DE
  1-0.38583+0.02432-18.2562+  0.907 -1.28474+0.04082
  2-0.20756+0.02028-26.7880+  1.446 -1.56401+0.06154
  3-0.35774+0.02085-26.3030+  1.731 -1.83234+0.08791
  4-0.46323+0.01841-20.9779+  1.063 -1.40250+0.04626
  5-0.52300+0.02110-10.2095+  0.607 -0.86886+0.02361
  6-0.51788+0.02297-11.4985+  0.674 -0.91529+0.02880
  7-0.39200+0.01098-16.1359+  0.566 -1.07576+0.02407

MEAN AND STD DEV BASED ON   7 SAMPLES
  7-0.40675+0.10127-18.5956+  6.083 -1.27764+0.32613
            24.9%            32.7%            25.5%

MEAN AND STD DEV BASED ON -  4 SAMPLES
  4-0.35359+0.09274-23.0813+  3.600 -1.52090+0.20533
            26.2%            15.6%            13.5%

MEAN AND STD DEV BASED ON +  3 SAMPLES
  3-0.47763+0.06059-12.6146+  2.545 -0.95330+0.08864
            12.7%            20.2%             9.3%
```

TABLE 13.   LONGITUDINAL   DERIVATIVE   ESTIMATES   AND   THEIR
CRAMÈR-RAO BOUNDS.

B - 2

```
      CZ DERIVATIVES
FACTOR ALPHA                    0                    DE
  1.0   -3.68751+0.08011 44.3280+   5.043 -2.45525+0.07534
        -3.47139+0.09503 96.2676+   7.589 -1.86384+0.08109

  1.5   -4.68977+0.09312-19.8944+   3.566 -2.27630+0.06688
        -4.62499+0.11889  9.7029+   5.200 -1.86261+0.07459

  1.9   -5.26684+0.11593-43.7695+   3.496 -2.24196+0.07280
        -5.31585+0.14331-20.0994+   4.726 -1.89297+0.07756



      CM DERIVATIVES
FACTOR ALPHA                    0                    DE
  1.0   -0.36369+0.01230-12.2338+   0.516 -0.90073+0.00609
        -0.34312+0.01404-10.8432+   0.756 -0.81520+0.00924

  1.5   -0.50713+0.01797-10.8547+   0.486 -0.91096+0.00633
        -0.47559+0.02214 -9.1165+   0.743 -0.82046+0.01019

  1.9   -0.61282+0.02505 -9.9973+   0.546 -0.91369+0.00753
        -0.57361+0.02987 -8.1401+   0.801 -0.82043+0.01139
```

TABLE 14.   LONGITUDINAL   DERIVATIVE   ESTIMATES   FOR   VARYING
UPWASH CORRECTION FACTORS (1.0, 1.5, AND 1.9).

B - 3

APPENDIX C

NOMENCLATURE

A   fundamental matrix

a_y lateral acceleration, positive right (g)

a_n normal acceleration ,positive down (g)

B   control effect matrix

C_l dimensionless rolling moment coefficient

C_m dimensionless pitching moment coefficient

C_n dimensionless yawing moment coefficient

C_X dimensionless axial force coefficient

C_Y dimensionless side force coefficient

C_Z dimensionless normal force coefficient

$\underline{c}$ vector of parameters to be estimated

$\underline{c}_o$ à priori value of $\underline{c}$

D1   instrument error weighting matrix

D2   à priori parameter estimate weighting matrix

$\underline{f}$ vector of nonlinear equations of motion

G,H   observation matrices

g   acceleration due to gravity (ft/sec^2)

I_x moment of inertia about the longitudinal axis (slug-ft^2)

I_Y moment of inertia about the lateral axis (slug-ft^2)

C - 1

I_Z moment of inertia about the normal axis (slug-ft^2)

I_{XY} cross-product of inertia about the longitudinal and lateral axes (slug-ft^2)

I_{XZ} cross-product of inertia about the longitudinal and normal axes (slug-ft^2)

I_{YZ} cross-product of inertia about the lateral and normal axes (slug-ft^2)

J   cost function

K   overall à priori weighting factor

L   likelihood function

L   rolling moment divided by moment of inertia about the longitudinal axis   (rad/sec^2)

M   pitching moment divided by moment of inertia about the lateral axis   (rad/sec^2)

m   aircraft mass (slugs)

N   yawing moment divided by moment of inertia about the normal axis   (rad/sec^2)   or number of sampling instants

$\underline{n}$ measurement errors vector

p   roll rate, perturbation

q   pitch rate, perturbation

R   acceleration transformation matrix

r	yaw rate, perturbation
S	reference area (ft^2)
u	longitudinal velocity, perturbation
$\underline{u}$	control deflections vector
V	velocity (ft/sec)
v	lateral velocity, perturbation
W	aircraft weight, (lb)
w	normal velocity, perturbation
$\underline{w}$	disturbances vector
X	longitudinal force divided by mass (ft/sec^2)
x	longitudinal position
$\underline{x}$	states vector
Y	side force divided by mass and velocity (rad/sec)
y	lateral position
$\underline{y}$	output vector
Z	normal force divided by mass and velocity (rad/sec)
z	normal position
$\underline{z}$	observation vector
α	angle-of-attack
β	sideslip angle
δa	aileron deflection, (right minus left)/2, (deg)
δe	elevator deflection from trim (deg)
δr	rudder deflection from fuselage centerline (deg)

δsf sideforce panel deflection, (right plus left)/2, (deg)

θ pitch angle (deg)

ϕ roll angle (deg)

ψ yaw angle (deg)

∇ gradient

REFERENCES

1.   Shivers, James P. , Fink, Marvin P. , and Ware, George
M. , "Full-Scale Wind-Tunnel Investigation of the Static
Longitudinal and Lateral Characteristics of a Light
Single-Engine Low-Wing Airplane," NASA TN D-5857, Jun. 1970.

2. Seckel, E. , and Morris, J. J. , "The Stability
Derivatives of the Navion Aircraft Estimated by Various
Methods and Derived From Flight Test Data," Rep. No.
FAA-RD-71-6, Jan. 1971.

3.   Suit, W. T. , "Aerodynamic Parameters of the Navion
Airplane Extracted From Flight Data," NASA TN-D 6643, Mar.
1972.

4.   Maine, R. E. and Iliff, K. W. , "A Fortran Program For
Determining Aircraft Stability And Control Derivatives From
Flight Data," TN-D-7831, Apr. 1975.

5. Etkin, B. , _Dynamics of Atmospheric Flight_, John Wiley
and Sons, Inc. , New York, 1972.

6. Maine, R.E. , "Maximum Likelihood Estimation of
Aerodynamic Derivatives For An Oblique Wing Aircraft From
Flight Data," AIAA Paper 77-1135, Aug. 1977.

7. Stepner, D. E.,and Mehra, R. K. , "Maximum Likelihood
Identification And Optimal Input Design For Identifying

Aircraft Stability And Control Derivatives," NASA CR-2200, Mar. 1973.

8. Iliff, K. W. and Taylor, L. W. , Jr. , "Determination of Stability Derivatives From Flight Data Using A Newton-Raphson Minimization Technique," NASA TN-D 6579, Mar. 1972.

9. Iliff, K. W, and Maine, R. E. , "Pratical Aspects of Using a Maximum Likelihood Estimator," AGARD CP 172, Nov. 1974.

10. Grove, R. D. , Bowles, R. L. , Mayhew, S. C. , "A Procedure For Estimating Stability And Control Parameters From Flight Test Data By Using Maximum Likelihood Methods Employing A Real-Time Digital System," NASA TN-D 6735, May 1972.

11. Balakrishnan, A. V. , Communications Theory. McGraw-Hill Book Co. , New York, 1968.

12. Brogan, W. L. , Modern Control Theory, Quantum Publishers, Inc. , New York, 1974.

13. Burgin, G. H. , "Two New Methods For Obtaining Stability Derivatives From Flight Test Data," NASA CR-96005, Sept. 1968.

14. Cannaday, R. L.,and Suit, W. T. , "Effects of Control Inputs on the Estimation of Stability and Control Parameters

of a Light Airplane," NASA Technical Paper 1403, Dec. 1977.

15. Mehra, R. K. , and Gupta, N. K. , "Status of Input Design Aircraft Parameter Identification," AGARD–CP–172, Nov. 1974.

16. Anon, <u>ASCOP Special Goodyear PW Ground Station,</u> Applied Science Corporation of Princeton, Oct. 1975.

17. Porter, F. H. , III, <u>Flight Data Reduction</u>, USAF Flight Test Center Publication T1'-700-1001, Jun. 1975.

18. Steers, S. T.,and Iliff, K. W. , "Effects of Time-Shifted Data on Flight-Determined Stability and Control Derivatives," NASA TN-D 7830, Mar. 1975.

19. Teper, Gary L. , "Aircraft Stability and Control Data," NASA CR-96008, Apr. 1969.